

Spatially Anisotropic Heisenberg Kagome Antiferromagnet

Andreas P. Schnyder,¹ Oleg A. Starykh,² and Leon Balents¹

¹*Kavli Institute for Theoretical Physics, University of California, Santa Barbara, CA 93106, USA*

²*Department of Physics, University of Utah, Salt Lake City, Utah 84112, USA*

(Dated: August 23, 2021)

We study the quasi-one-dimensional limit of the spin-1/2 quantum Heisenberg antiferromagnet on the kagome lattice. The lattice is divided into antiferromagnetic spin-chains (exchange J) that are weakly coupled via intermediate “dangling” spins (exchange J'). Using one-dimensional bosonization, renormalization group methods, and current algebra techniques the ground state is determined in the limit $J' \ll J$. We find that the dangling spins and chain spins form a spiral with $O(1)$ and $O(J'/J)$ static moments, respectively, atop of which the chain spins exhibit a smaller $O[(J'/J)^2]$ antiferromagnetically ordered component along the axis perpendicular to the spiral plane.

I. INTRODUCTION

The nearest-neighbor Heisenberg antiferromagnet on the kagome lattice, a two-dimensional network of corner-sharing triangles, is one of the most geometrically frustrated magnets. Frustration suppresses the magnetic ordering tendency and leads to an extensive classical ground state degeneracy. Order-by-disorder effects lift the degeneracies in the classical system and are believed to select the coplanar $\sqrt{3} \times \sqrt{3}$ pattern as the ground state.^{1,2,3,4}

The spin-1/2 quantum kagome antiferromagnet is much less understood. Exact diagonalization^{5,6,7,8,9,10,11} and series expansion studies^{12,13} indicate the absence of long-range magnetic order, but the precise nature of the ground state remains mysterious. For small systems, numerical simulations reveal a large number of singlet states below a small (and possibly vanishing) spin gap.^{8,9,14} This observation has led to the speculation that the ground state of the kagome lattice might be a gapless critical spin liquid^{15,16,17} or a particular type of valence-bond crystal that exhibits many low-energy singlet states^{18,19,20} (see also Refs. 21 and 22).

Recently, two new candidate materials for an ideal spin-1/2 kagome antiferromagnet have attracted considerable attention. First, the mineral $\text{ZnCu}_3(\text{OH})_6\text{Cl}_2$, also known as Herbertsmithite, realizes structurally undistorted, magnetically isolated kagome layers with Cu^{2+} moments on the lattice sites.^{23,24,25,26,27,28,29} Neither magnetic ordering nor spin freezing has been observed for this material down to the lowest currently achievable temperature of 50 mK, which is well below the energy scale of the antiferromagnetic interaction.^{24,25,26} While Herbertsmithite is structurally perfect, Dzyaloshinskii-Moriya (DM) interactions and a small number of impurities might complicate the experimental study of the ideal quantum kagome system.³⁰ Secondly, there is Volborthite $\text{Cu}_3\text{V}_2\text{O}_7(\text{OH})_2 \cdot 2\text{H}_2\text{O}$, a spin-1/2 (Cu^{2+}) antiferromagnet, whose magnetic sublattice consists of well-separated kagome-like planes.^{31,32,33,34} This material has a monoclinic distortion, which deforms the equilateral kagome triangles into isosceles triangles leading to a difference between two of the nearest-neighbor exchange constants (J') and the third one (J). Similarly as in Herbertsmithite, the spins do not order down to 1.8 K, an energy scale fifty times smaller than the exchange coupling strength in Volborthite.³¹ However, at very low tem-

peratures evidence for a spin freezing transition has been reported.³⁴ The anisotropy ratio of the exchange couplings, $\alpha = J/J'$, could not be determined experimentally so far, but the differing side lengths of the kagome triangles seem to favor $\alpha > 1$. A recent comparison of exact diagonalization calculations with thermodynamic measurements suggests that the spatial anisotropy of the exchange couplings is small, and that additional interactions beyond the nearest-neighbor couplings might be present in the mineral Volborthite.³⁵

In this paper, motivated by the renewed interest in the kagome systems and the recent experiments on Volborthite, we investigate the spatially anisotropic version of the quantum kagome antiferromagnet. We shall focus on the quasi-one-dimensional limit, $J' \ll J$, where the model consists of quantum-critical spin-1/2 chains weakly coupled together via intermediate “dangling” spins (see Fig. 1). In this situation the competition between quantum fluctuations and the strong geometric frustration of the kagome lattice is particularly keen. The anisotropic quantum kagome antiferromagnet has been studied previously by a variety of techniques, all of which employ perturbation theories in some “artificial” small parameter. Examples include large- N expansions of the $\text{Sp}(N)$ symmetric generalization of the model,^{36,37} a block-spin perturbation approach to the trimerized kagome lattice,³⁷ and semiclassical calculations in the limit of large spin.^{37,38} Our approach is complementary to these studies in that it offers a fairly controlled analysis of the quasi-one-dimensional limit using powerful field-theoretical methods^{39,40,41} that have originally been developed for the investigation of quantum critical systems in one dimension. Recently, the quasi-one-dimensional version of the kagome antiferromagnet in a strong magnetic field, assuming that the intermediate spins are fully polarized, has been studied using similar techniques.⁴² The present paper treats the case of zero external field.

Our approach rests on the assumption that in the quasi-one-dimensional limit, $J' \ll J$, the intermediate spins order at a temperature scale T_s much higher than the ordering temperature T_{ch} of the weakly coupled chains. This is justified a posteriori by our finding that the effective interaction among the interstitial spins, which sets the temperature scale T_s , is of order $(J')^2/J$, whereas the most relevant effective interaction among the weakly coupled spin-1/2 chains, which determines T_{ch} , is of order $(J')^4/J^3$. Consequently, we can divide the

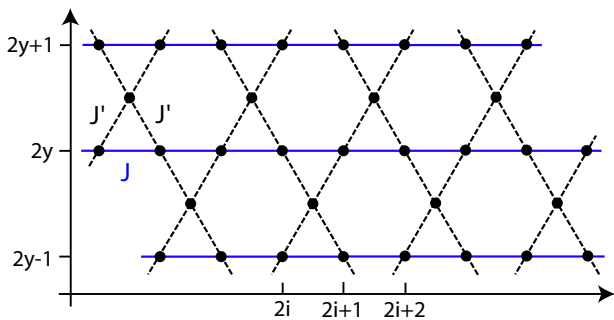


FIG. 1: (Color online) Spatially anisotropic kagome lattice with nearest-neighbor exchange J (blue) among chain spins (S) and J' (black) among chain spins and interstitial spins (s).

theoretical analysis into three separate stages. First, we derive the effective interaction among the intermediate dangling spins using perturbative renormalization group (RG) transformations in the time direction. These considerations are complemented by numerical estimates of the induced short distance couplings among the dangling spins. Second, we analyze the ground state of the resulting, spatially anisotropic triangular lattice of dangling spins as a function of first and further-neighbor interactions. We find that in the ground state the interstitial spins form a rotating spiral with a small (and possibly vanishing) wave vector parallel to the chain direction. Third we determine the most relevant interchain interactions using a symmetry analysis and RG considerations. Besides the effective interchain interaction, the spiral magnetic field produced by the intermediate spins induces another perturbation to the system of decoupled Heisenberg chains. Finally, we analyze these perturbations to the fixed point of the independent (decoupled) spin-1/2 chains with the help of operator product expansions (OPEs).

The ultimate result of our analysis is that all spins order, with the non-coplanar configuration shown in Fig. 2, in which the interstitial and chain spins predominantly form coplanar spirals with a wave vector $(q, 0)$, but with a reduced $O(J'/J)$ static moment on the chains. The chain spins are weakly canted out of the plane, with the $O[(J'/J)^2]$ normal components forming an antiferromagnetically ordered pattern. The precise value of q cannot be reliably determined from our analysis, but we expect $q \ll 1$ and $q = 0$ is a distinct possibility. In the $q = 0$ case, the state becomes coplanar. This ordered state differs from those found in two other recent studies^{37,38} using other methods, but there are similarities. These are discussed in Sec. VII.

At first glance, it might be counter-intuitive that the interstitial spins and the chain spins order in a nearly ferromagnetic fashion among themselves rather than in an antiferromagnetic pattern. But it has to be kept in mind that the ordering of the quasi-one-dimensional version of the kagome antiferromagnet is driven by the weakly coupled interstitial spins, which order at a larger energy scale than the chain spins. There is no a priori reason that the effective interaction among the interstitial spins should be purely antiferromagnetic. In fact, it turns out

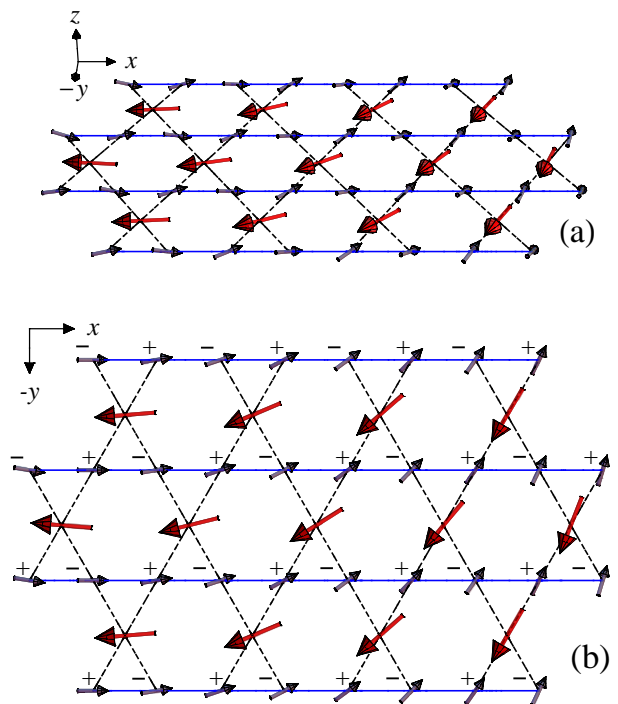


FIG. 2: (Color online) (a) Three-dimensional perspective view of the spin ordering pattern. The interstitial spins (red arrows) form a coplanar spiral with an $O(1)$ local moment in the x - y plane. The components of the chain spins (gray arrows) in the x - y plane also form a spiral but with static moment of $O[J'/J]$ and antiparallel to the interstitial spins. The out-of-plane components (z direction) of the chain spins are non-zero but even smaller – $O[(J'/J)^2]$ – and ordered antiferromagnetically along and between the chains. (b) Top view of the spin ordering pattern. The vertical component of the chain spins is indicated using + (upward pointing) and – (downward pointing).

that there is an effective *ferromagnetic* interaction along the diagonal bonds connecting nearest neighbor interstitial spins (see Sec. IV). Together with an effective antiferromagnetic interaction along the horizontal bonds connecting neighboring interstitial spins this ultimately leads to the spiral order of the dangling spins. The spiral order of the chain spins can then be understood as arising from the linear response to the local field of the ordered interstitial moments.

The remainder of the paper is organized as follows. Sec. II describes the lattice Hamiltonian, its symmetries, and its low-energy field theory description. In Sec. III we analyze the low-energy interactions using symmetry considerations and a perturbative renormalization treatment. In Sec. IV we use numerical methods to estimate the interaction strength among the interstitial spins and derive an effective model for the dangling spins on the triangular lattice. Sec. V deals with the ground state analysis of the triangular lattice. The perturbative analysis of weakly coupled chains in a spiral magnetic field with a small wave vector, $q \ll 1$, is presented in Sec. VI and our conclusions and a discussion of the relation to other results are given in Sec. VII. Some technical aspects of the RG calculations are relegated to Appendix A. For completeness,

we study in Appendix B the ordering of the weakly coupled chains in the presence of a spiral field with a large wave vector.

II. MODEL DEFINITION AND LOW-ENERGY HAMILTONIAN

The Hamiltonian of the Heisenberg antiferromagnet on the anisotropic kagome lattice (see Fig. 1) is given by $H = H_0 + V$, where H_0 describes the decoupled set of chains with nearest-neighbor antiferromagnetic Heisenberg interactions

$$H_0 = J \sum_{i,y} \mathbf{S}_{i,y} \cdot \mathbf{S}_{i+1,y}, \quad (1a)$$

and V is the interaction among the chains and the intermediate spins

$$V = J' \sum_{i,y} \mathbf{s}_{2i \pm \frac{1}{2}, 2y \mp \frac{1}{2}} \cdot \left(\mathbf{S}_{2i, 2y} + \mathbf{S}_{2i \pm 1, 2y} + \mathbf{S}_{2i, 2y \mp 1} + \mathbf{S}_{2i \pm 1, 2y \mp 1} \right). \quad (1b)$$

For the interstitial spins we shall use the symbol \mathbf{s} , whereas the chain spins are denoted by \mathbf{S} . The anisotropic kagome lattice has rotation, translation and reflection symmetries. The translational subgroup is generated by the translations T_1 and T_2 , which move the lattice by two units along the horizontal, and one of the diagonal axes, respectively. The rotational subgroup consists of π rotations about the lattice sites and about the centers of the hexagons. We can distinguish two types of reflection symmetries: reflections R_1 about a vertical line through a midpoint of a chain bond (link parity), and reflections R_2 about a horizontal line passing through the intermediate dangling spins (see Fig. 1).

Let us now describe the chains in the continuum limit, which is applicable as long as $J \gg J'$. In this limit the low-energy properties of the antiferromagnetic spin-1/2 chains are governed by the Wess-Zumino-Novikov-Witten (WZNW) $SU(2)_1$ theory, and the chain spin operator $\mathbf{S}_{i,y}$ can be decomposed into its uniform $\mathbf{M}_y(x)$ and staggered $\mathbf{N}_y(x)$ spin magnetizations

$$\mathbf{S}_{i,y} \rightarrow a_0 [\mathbf{M}_y(x) + (-1)^x \mathbf{N}_y(x)], \quad (2a)$$

where $x = ia_0$ and a_0 denotes the lattice spacing. The uniform magnetization can be written in terms of left- and right-moving $SU(2)$ currents, $\mathbf{M}_y = \mathbf{J}_{y,R} + \mathbf{J}_{y,L}$. Another important operator describing low energy properties of the spin-1/2 chains is the staggered dimerization $\varepsilon_y(x)$, which is defined as the continuum limit of the scalar product of two neighboring spins

$$\mathbf{S}_{i,y} \cdot \mathbf{S}_{i+1,y} \rightarrow (-1)^x \varepsilon_y(x). \quad (2b)$$

The scaling dimension of these continuum operators determines the relevance of the operator in the RG sense with respect to the Luttinger liquid fixed point of the decoupled

chains. The uniform magnetization \mathbf{M}_y has scaling dimension 1, whereas both the staggered spin magnetization \mathbf{N}_y and the staggered dimerization ε_y have scaling dimension 1/2. The microscopic lattice symmetries of H , Eq. (1), leave an imprint on continuum description (2). That is, the action of the space group symmetries on the continuum operators is given by

$$T_1 : \quad \mathbf{M} \rightarrow \mathbf{M}, \quad \mathbf{N} \rightarrow +\mathbf{N}, \quad \varepsilon \rightarrow +\varepsilon, \quad (3a)$$

$$R_1 : \quad \mathbf{M} \rightarrow \mathbf{M}, \quad \mathbf{N} \rightarrow -\mathbf{N}, \quad \varepsilon \rightarrow +\varepsilon, \quad (3b)$$

$$R_2 \circ T_2 : \quad \mathbf{M} \rightarrow \mathbf{M}, \quad \mathbf{N} \rightarrow -\mathbf{N}, \quad \varepsilon \rightarrow -\varepsilon, \quad (3c)$$

where, for brevity, we have suppressed the chain index. Other symmetry operations on the continuum fields are either trivial, or can be rewritten as a product of the above transformations.

The three continuum fields \mathbf{M} , \mathbf{N} , and ε form a closed operator algebra with respect to certain operator product expansions, which are widely used in the literature.^{39,40,41,43,44,45,46} For example, the right-moving $SU(2)$ currents \mathbf{J}_R satisfy the following chiral OPEs

$$J_R^a(x, \tau) J_R^b(0) = \frac{\delta^{ab}/(8\pi^2)}{(u\tau - ix + a_0\sigma_\tau)^2} + \frac{i\varepsilon^{abc} J_R^c(0)/(2\pi)}{u\tau - ix + a_0\sigma_\tau}, \quad (4a)$$

with imaginary time τ , $\sigma_\tau = \text{sgn } \tau$, the short-distance cut-off a_0 , and spin velocity $u = \pi J a_0/2$. Similar relations hold for the left-moving spin currents \mathbf{J}_L . The product of \mathbf{J}_R and \mathbf{N} can be expanded as

$$J_R^a(x, \tau) N^b(0) = \frac{i\varepsilon^{abc} N^c(0) - i\delta^{ab}\varepsilon(0)}{4\pi(u\tau - ix + a_0\sigma_\tau)}. \quad (4b)$$

The above equalities are understood to be valid only when inserted into correlation functions and in the limit where the two points (x, τ) and $(0, 0)$ are close together. These current algebra relations will allow us to compute one-loop RG equations by purely algebraic means (see Secs. III and VI).

Using relation (2a), we can derive a naive continuum limit of the interaction among the chains and the intermediate spins, Eq. (1b). First, we note that the intermediate spins $\mathbf{s}_{2i \pm \frac{1}{2}, 2y \mp \frac{1}{2}}$ couple symmetrically to $\mathbf{S}_{2i, 2y}$ and $\mathbf{S}_{2i \pm 1, 2y}$. Hence, the staggered spin magnetization enters only via its first derivative in the continuum version of the interaction V , and we can set

$$\mathbf{S}_{2i, 2y} + \mathbf{S}_{2i \pm 1, 2y} \rightarrow 2a_0 \mathbf{M}_{2y}(2x) - \frac{a_0^2}{2} \partial_x \mathbf{N}_{2y}(2x). \quad (5)$$

In the above, and the following, we use the notation that the derivative in $\partial_x \mathbf{N}_{2y}(2x)$ is with respect to the full argument, i.e., more explicitly

$$\partial_x \mathbf{N}_{2y}(2x) \equiv \partial_X \mathbf{N}_{2y}(X)|_{X=2x}. \quad (6)$$

With this, the interaction Eq. (1b) reads $V = V_1 + V_2$, with

$$V_1 = \gamma_1 \sum_{x,y} \mathbf{s}_{2x \pm \frac{1}{2}, 2y \mp \frac{1}{2}} \cdot [\mathbf{M}_{2y}(2x) + \mathbf{M}_{2y \mp 1}(2x)], \quad (7)$$

$$V_2 = \gamma_2 \sum_{x,y} (\pm) \mathbf{s}_{2x \pm \frac{1}{2}, 2y \mp \frac{1}{2}} \cdot \partial_x [\mathbf{N}_{2y}(2x) + \mathbf{N}_{2y \mp 1}(2x)],$$

where the bare coupling constants are given by, $\gamma_1 = 2J'a_0$ and $\gamma_2 = -J'a_0^2/2$, which follows from substituting (5) into (1b). We have retained the next-to-leading interaction V_2 as it will produce, in combination with the leading term V_1 , relevant interchain couplings with respect to the fixed point of the decoupled chains (see Sec. III). The continuum description of the interaction V , Eq. (7), is necessarily invariant under the symmetry transformations, Eq. (3). In particular, we note that V does not contain a contribution $\mathbf{s}_{2x+\frac{1}{2},2y-\frac{1}{2}} \cdot \mathbf{N}_{2y}(2x)$ which is forbidden by the symmetries of the spatially anisotropic kagome lattice (link parity R_1 sends $\mathbf{N} \rightarrow -\mathbf{N}$).

III. RENORMALIZATION GROUP TREATMENT

Here, we study the effective low-energy interactions among the dangling spins (H_Δ), as well as those between nearest neighbor chains (V_{ch}), using both a symmetry analysis and perturbative renormalization group transformations. The goal is to understand which interactions amongst interstitial spins, amongst chains, or betwixt the two, are most relevant, and further, at what energy scales they become important in determining the low-energy physics. Technically, the Hamiltonian (1) with the chains treated in the continuum limit is formally rather similar to a Kondo lattice. As the Hamiltonian retains some local character due to the intermediate spins, in the framework of the RG approach, this problem develops only in time, and the energy is the only variable that is being rescaled as the RG progresses. Such an RG scheme is similar in spirit to the one employed in the context of a single impurity coupled to a Luttinger liquid (see, for example, Refs. 47,48,49).

A. Symmetry analysis

Before proceeding with the RG derivation of the low-energy effective interactions, we first write down the most general form of V_{ch} and H_Δ that are allowed by the symmetries of the spatially anisotropic kagome lattice. Such a general symmetry consideration will reveal all relevant symmetry allowed interactions that are expected to be generated through RG transformations, when all nominally irrelevant terms are taken into account. The space group symmetries needed for this analysis have been discussed in Sec. II [see Eqs. (3)].

We begin with the interchain Hamiltonian V_{ch} . In principle, the number of allowed interchain interaction terms is infinite. However, only a handful of terms will be important. Most significant are those terms which are most relevant in the RG sense (with respect to the Luttinger liquid fixed point of the decoupled chains). This amounts to two-chain interactions involving no derivatives and only continuum fields that have small scaling dimension. Amongst these, we may further restrict ourselves to nearest-neighbor chain interactions, as the magnitude of further-neighbor chain interactions is expected to decrease with separation distance. The continuum operators with the smallest scaling dimension are the staggered

dimerization ε_y and the staggered magnetization N_y . Therefore, we find

$$V_{\text{ch}} = \sum_y \int dx \{ \gamma_N \mathbf{N}_y \cdot \mathbf{N}_{y+1} + \gamma_\varepsilon \varepsilon_y \varepsilon_{y+1} \}, \quad (8)$$

where the value of the coupling constants γ_N and γ_ε will have to be determined by microscopic calculations. Using Eqs. (3) it is straightforward to check that these are the only terms with lowest possible scaling dimension 1 that satisfy the symmetry requirements of the spatially anisotropic kagome lattice.

In addition to these most relevant interchain interactions, it is necessary to consider also a few less relevant terms, as these will arise at lower order in the renormalization group treatment below, and are important for *generating* the more relevant terms in Eq. (8) above. These are

$$V_{\text{ch}}^{(1)} = \sum_y \int dx \{ \gamma_{\partial N} \partial_x \mathbf{N}_y \cdot \partial_x \mathbf{N}_{y+1} + \gamma_M \mathbf{M}_y \cdot \mathbf{M}_{y+1} \}. \quad (9)$$

Next, we turn to interactions among the interchain spins H_Δ . Considering only terms that arise at $O[(J')^2]$, we find that H_Δ is given by Heisenberg interactions among dangling spins whose y coordinates differ by at most one unit. The coupling constants of these Heisenberg interactions are restricted by the symmetries of the lattice. With these conditions, H_Δ can be conveniently written in the form (see Fig. 3)

$$H_\Delta = \sum_{x,y,r>0} \mathcal{J}_{2r} \mathbf{s}_{2x\pm\frac{1}{2},2y\mp\frac{1}{2}} \cdot \mathbf{s}_{2x\pm\frac{1}{2}+2r,2y\mp\frac{1}{2}} \quad (10)$$

$$+ \sum_{x,y,r} \mathcal{J}_{|2r+1|} \mathbf{s}_{2x\pm\frac{1}{2},2y\mp\frac{1}{2}} \cdot \mathbf{s}_{2x\pm\frac{3}{2}+2r,2y\pm\frac{1}{2}}.$$

Since the couplings J_r decrease in magnitude with increasing $|r|$, we can truncate the above sums over r after the first few terms.

B. Renormalization group results

To determine the fluctuation-generated corrections to the low-energy effective action we perform a perturbative RG analysis of the interactions V , Eq. (7), to one-loop order. The perturbation theory is formulated by expanding the partition function $Z = \int e^{-S_0 - \int d\tau V}$ up to quadratic order in the couplings

$$Z \simeq \int e^{-S_0} \left[1 - \int d\tau V + \frac{1}{2} \text{T} \int d\tau_1 d\tau_2 V(\tau_1) V(\tau_2) \right]. \quad (11)$$

Here, S_0 denotes the fixed point action, T is the time-ordering operator, and τ_i is the imaginary time. Implicit in Eq. (11) is a regularization, such that the integrals appearing in the expansion are taken only over the regions in which no two times are closer than some short time cut-off $\alpha = a_0/u$. The RG proceeds by increasing this cut-off infinitesimally from α to $b\alpha$, where $b = e^{d\ell}$ and $d\ell > 0$ is the usual logarithmic change of scale. To do this, all pairs of times τ_1, τ_2 such

that $\alpha < |\tau_1 - \tau_2| < b\alpha$ must be fused using the operator product expansion, and the integral over $\tau_1 - \tau_2$ in this range carried out. One thereby obtains a new partition function with renormalized interactions and the increased cut-off. We then perform an additional trivial rescaling of time and space coordinates for to restore the original cut-off:

$$\begin{aligned} \mathbf{N}_y(x, \tau) &\rightarrow b^{-1/2} \mathbf{N}_y(x/b, \tau/b), \\ \mathbf{M}_y(x, \tau) &\rightarrow b^{-1} \mathbf{M}_y(x/b, \tau/b), \\ \mathbf{s}_{x,y}(\tau) &\rightarrow \mathbf{s}_{x,y}(\tau/b). \end{aligned} \quad (12)$$

We note that the spatial rescaling is not required to restore the cut-off but is natural and convenient for the continuum fields of the chains, which are described by a Lorentz invariant field theory. By contrast, we obviously cannot rescale the coordinates of the discrete spin operators of the interstitial spins. This difference leads to the appearance of an explicit RG length scale in the effective couplings between the chains and interstitial spins, V_1 and V_2 , in the renormalized Hamiltonian:

$$\begin{aligned} V_1(\ell) &= \gamma_1 \sum_{x,y} \mathbf{s}_{2x \pm \frac{1}{2}, 2y \mp \frac{1}{2}} \cdot [M_{2y}(2x_\ell) + M_{2y \mp 1}(2x_\ell)], \\ V_2(\ell) &= \gamma_2 \sum_{x,y} (\pm) \mathbf{s}_{2x \pm \frac{1}{2}, 2y \mp \frac{1}{2}} \cdot \partial_x [N_{2y}(2x_\ell) \\ &\quad + N_{2y \mp 1}(2x_\ell)], \end{aligned} \quad (13)$$

where $x_\ell = xe^{-\ell}$.

With this, the derivation of the RG equations is straightforward, and follows closely the methods used in Refs. 47,48,49. Details of the calculations can be found in Appendix A. Taking into account $V = V_1 + V_2$ to one loop, we obtain RG equations for both the interchain couplings and the couplings between the interstitial spins. The former are

$$\begin{aligned} \frac{d\gamma_1}{d\ell} &= +\frac{1}{\pi u} \gamma_1^2, & \frac{d\gamma_2}{d\ell} &= -\frac{1}{2} \gamma_2 + \frac{1}{\pi u} \gamma_1 \gamma_2, \\ \frac{d\gamma_{\partial N}}{d\ell} &= -\gamma_{\partial N} - \frac{\gamma_2^2}{u}, & \frac{d\gamma_M}{d\ell} &= -\gamma_1^2 + \frac{\gamma_M^2}{2\pi u}, \\ \frac{d\gamma_N}{d\ell} &= \gamma_N + \frac{\gamma_{\partial N} \gamma_M}{8\pi \alpha^2 u}, & \frac{d\gamma_\epsilon}{d\ell} &= \gamma_\epsilon - \frac{3\gamma_{\partial N} \gamma_M}{16\pi \alpha^2 u}. \end{aligned} \quad (14)$$

Note that the strongly relevant interactions $\gamma_N, \gamma_\epsilon$ are *not* generated at one loop from γ_1, γ_2 . Instead, the former are generated from the sub-dominant $\gamma_{\partial N}, \gamma_M$ terms. This is the reason the latter terms needed to be included in our treatment.

The RG equations for the interstitial spin couplings are *functional*, insofar as they describe the flow of the full set of interactions \mathcal{J}_r . We find

$$\frac{d\mathcal{J}_{2r}}{d\ell} = \mathcal{J}_{2r} + I_M(re^{-\ell}) \frac{\gamma_1^2}{u} + I_N(re^{-\ell}) \frac{\gamma_2^2}{u}, \quad (15a)$$

where

$$\begin{aligned} I_M(r) &= \sum_{\sigma'=\pm 1} \frac{\alpha}{4\pi^2} \frac{1}{[\alpha + \sigma' i 2r]^2}, \\ I_N(r) &= 8C_N \frac{\alpha(\alpha^2 - 8r^2)}{(\alpha^2 + 4r^2)^{5/2}}, \end{aligned} \quad (15b)$$

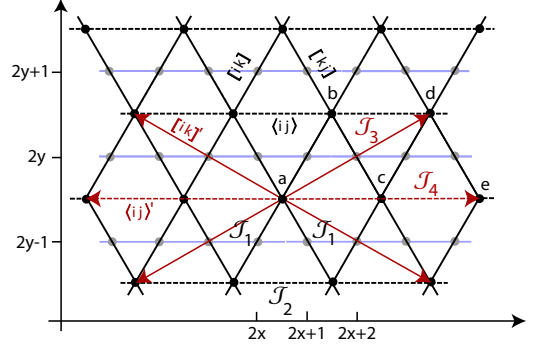


FIG. 3: (Color online) Exchange paths of the triangular lattice formed by the intermediate spins s of the spatially anisotropic kagome lattice. Solid black lines denote the nearest-neighbor ferromagnetic exchange \mathcal{J}_1 (a - b and b - c bonds), dotted black lines the nearest-neighbor antiferromagnetic exchange \mathcal{J}_2 (a - c bond). The further neighbor interactions \mathcal{J}_3 (a - d bond) and \mathcal{J}_4 (a - e bond) for the spin s_a are illustrated with red arrows. The chain bonds of the anisotropic kagome lattice are indicated in light blue (cf. Fig. 1).

where C_N is the amplitude of the $\langle N^a N^a \rangle$ correlator. Analogous expressions can be derived for the interactions $\mathcal{J}_{|2r+1|}$, i.e., the second term in H_Δ , Eq. (10).

In passing, we note that the form of the RG flows in Eqs. (14) is highly constrained by the symmetry of the full (spatially anisotropic) kagome lattice, and this is necessary to avoid the generation of strongly relevant interactions at this order. By contrast, for the kagome *strip* of extension one in the y direction, there is no translational symmetry T_2 , and consequently symmetry (3c) is absent. This allows for the appearance of a term in the renormalized Hamiltonian proportional to $\int dx \varepsilon_y(x, \tau)$, which is indeed generated proportionally to $\gamma_1 \gamma_2$ in that case (compare with Azaria *et al.*, Ref. 50, and see Ref. 51). This term is strongly relevant and generates a gapped dimerized state in that model.

C. Implications

The RG flows in Eqs. (14,15) give considerable insight into the emergent energy scales in the problem. Though interactions between the chains and between the interstitial spins are both generated from the bare interactions γ_1, γ_2 , their characters are distinctly different. Crucially, we see from Eqs. (14) that amongst the chains, only marginal and irrelevant interactions $-\gamma_{\partial N}, \gamma_M$ are generated at this order. Since the bare values $\gamma_1(\ell=0) \sim \gamma_2(\ell=0)$ are both of $O[J']$, this includes all effective generated interactions up to $O[(J')^2]$. A simple scaling argument shows that the low-energy excitations of the chains can be modified from those of decoupled chains only on energy scales *parametrically smaller* than $(J')^2$.

To understand this, let us consider the solutions to Eqs. (14) in somewhat more detail. The most important observation is that the strongly relevant interactions, $\gamma_N, \gamma_\epsilon$ [third line of Eqs. (14)], once they are generated, grow rapidly and expo-

nentially with ℓ . They are therefore dominated by the effects of their “source” terms (proportional to $\gamma_{\partial N} \gamma_M$) at small ℓ , which are most amplified under the growth. The source terms at small scale are themselves of order $(J')^2/J$, as described above. Therefore we expect that the relevant interactions will be, at least until they renormalize to large values, of order $(J')^4/J^3$. Indeed, the ultimate effect of all this short-scale renormalization is completely equivalent to including fluctuation-generated “bare” interactions of this same order. This procedure has been described in considerable detail in prior publications, in which the formal manipulations closely parallel those used here. See Refs. 39,41 for further information. Therefore we will in Sec. VI simply take the relevant couplings to have the appropriate values:

$$\gamma_N(\ell \sim 1) = +\frac{2(J')^4}{4\pi^4 J^3}, \quad \gamma_\varepsilon(\ell \sim 1) = -\frac{3(J')^4}{4\pi^4 J^3}. \quad (16)$$

By contrast, the interactions \mathcal{J}_r generated in Eqs. (15) at $O[(J')^2]$ amongst the dangling spins will clearly modify their energetics at this same order, since they act within an otherwise completely degenerate manifold. More formally, this follows directly from the RG flows, Eq. (15), which shows that the interstitial interactions will grow to $O(1)$ values (actually to any fixed value) by a scale $J e^\ell \sim J(\gamma_1^2, \gamma_2^2) \sim (J')^2/J$. Therefore we see that, as claimed in the introduction, the ordering (as we shall see, this is the result of these interactions) of the interstitial spins occurs at an energy scale at which the chains are unaffected by their couplings to the interstitial spins and each other.

Having understood the hierarchy of energy scales resulting from the RG, we can proceed to try to understand in more detail the ordering of the interstitial spins. In principle, one may do so by integrating the flow equations for the \mathcal{J}_r couplings, Eqs. (15), from $\ell = 0$ to the ordering scale, $\ell = 2 \ln(J/J')$. This is equivalent to performing the time integrals not over the infinitesimal shell in the vicinity of the running cut-off, but instead from microscopic times α up to times of order $\alpha(J/J')^2$. Inspection of expressions in Eq. (15b) shows that these integrals in fact are dominated by times of order the microscopic time. Indeed the upper limit of the time integration can be extended to infinity without significant modification of the result.

The dominance of short times has physical significance: it implies that the generated interstitial spin interactions are in fact controlled by high-energy physics of the Heisenberg chains, i.e., correlations of the chain spins on the scale of a few lattice spacings. These short distance correlations are *not* precisely captured by the continuum bosonization/current algebra approach. Therefore, if an accurate determination of these dangling spin interactions is desired, we must abandon (for the moment) the field theory methodology and return to a direct study of the lattice model. Conversely, because the generated interactions are dominated by short distance physics, we expect that no serious divergences will arise in a microscopic calculation. In the following section we show how perturbative and numerical methods may be used to perform the necessary calculations and obtain the fluctuation generated interactions amongst the interstitial spins. Using these precise

results we determine the interstitial spin ordering in Sec. V.

Following this, in Sec. VI we will return to the lower energy physics resulting from the fluctuation-generated interactions $\gamma_{\partial N}, \gamma_M$ in Eqs. (14), which will ultimately lead to ordering amongst the chain spins as well.

IV. NUMERICAL ESTIMATES OF INTERACTIONS AMONG DANGLING SPINS

The dynamical structure factor of the spin-1/2 antiferromagnetic Heisenberg chain, $S(q, \omega)$, can be related to the coupling constants of the effective interactions among the dangling spins, \mathcal{J}_r , by means of second-order degenerate perturbation theory in the interaction V , Eq. (1b). Using available numerical data for $S(q, \omega)$, both in the two-spinon approximation and for finite-size systems, this gives an estimate for the sign and relative strength of the interactions \mathcal{J}_r .

To formulate the perturbation theory in V we denote the ground state of the unperturbed Hamiltonian H_0 , Eq. (1a), by $|0\rangle$ and introduce the ground-state projection operator $P = |0\rangle\langle 0|$. With $Q = 1 - P$, any given state $|\Psi\rangle$ of chain (\mathbf{S}) and interchain (\mathbf{s}) spins can be written as $|\Psi\rangle = |\Psi_0\rangle + |\Psi_Q\rangle$, where $|\Psi_0\rangle = P|\Psi\rangle$ and $|\Psi_Q\rangle = Q|\Psi\rangle$. We note that $|\Psi_0\rangle$ describes the state with the chain spins in the ground state, while the state of the \mathbf{s} -spins remains arbitrary, i.e., $|\Psi_0\rangle = |0\rangle|\{\mathbf{s}\}\rangle$. Following along the lines of Refs. 42,52, we obtain an eigenvalue equation for $|\Psi_0\rangle$

$$\left(H_0 + PV \frac{1}{1 - RQV} RV\right) |\Psi_0\rangle = E |\Psi_0\rangle, \quad (17)$$

with the resolvent $R = (E - H_0)^{-1}$. Eq. (17) is highly nonlinear in the energy E , since the left-hand side of this equation depends on E through the resolvent R . Performing a perturbation expansion on the operator $(1 - RQV)^{-1}$ gives at second order in J'

$$\left(H_0 + PVR_0V\right) |\Psi_0\rangle = E |\Psi_0\rangle, \quad (18)$$

where $R_0 = (E_0 - H_0)^{-1}$ is a function of the ground state energy E_0 of the decoupled chains. Multiplying Eq. (18) from the left by $\langle 0|$ and inserting the perturbation V , Eq. (1b), yields, after some algebra, a Schrödinger equation for the interchain spins alone

$$H_\Delta |\{\mathbf{s}\}\rangle = (E - E_0) |\{\mathbf{s}\}\rangle, \quad (19a)$$

with the effective interaction among interstitial spins

$$H_\Delta = 4(J')^2 \sum_{x,y,r>0} A(2r) \left[\mathbf{s}_{2x \pm \frac{1}{2}, 2y \mp \frac{1}{2}} \cdot \mathbf{s}_{2x \pm \frac{1}{2} + 2r, 2y \mp \frac{1}{2}} \right] \\ + 2(J')^2 \sum_{x,y,r} A(|2r + 1|) \left[\mathbf{s}_{2x \pm \frac{1}{2}, 2y \mp \frac{1}{2}} \cdot \mathbf{s}_{2x \pm \frac{3}{2} + 2r, 2y \pm \frac{1}{2}} \right]. \quad (19b)$$

Here, $A(r)$ is the linear combination

$$A(r) = G_M(r - 1) + 2G_M(r) + G_M(r + 1) \quad (20)$$

of the ground state expectation values

$$G_M(r) = \langle 0 | S_{2x,y}^a \frac{1}{E_0 - H_0} S_{2x+r,y}^a | 0 \rangle. \quad (21)$$

In deriving equation (19) we made use of the fact that the expectation value (21) is independent of both the x and y coordinates, due to translational invariance. The linear combination in Eq. (20) arises, because every interstitial spin s is coupled to pairs of chain spins S . From inspection of Eq. (19) we find the following expressions for the exchange couplings \mathcal{J}_r , which have been defined in Eq. (10),

$$\begin{aligned} \mathcal{J}_{2r} &= 4(J')^2 A(2r), \\ \mathcal{J}_{2r+1} &= 2(J')^2 A(2r+1), \end{aligned} \quad (22)$$

with $r > 0$. The factor of 2 difference between the first and the second lines in Eq. (22) accounts for the fact that interstitial spins s with the same y coordinate, say, $y - \frac{1}{2}$, are connected via both the y and $y - 1$ chains.

Finally, by inserting a resolution of identity in Eq. (21),

$$G_M(r) = \sum_{n \neq 0} \langle 0 | S_{2x,y}^a | n \rangle \frac{1}{E_0 - E_n} \langle n | S_{2x+r,y}^a | 0 \rangle,$$

with $|n\rangle$ denoting the eigenstates of H_0 , we realize that $G_M(r)$, Eq. (21), is just a spectral representation of the zero-frequency Matsubara spin Green's function

$$G_M(r) = - \int_0^\infty d\tau \langle T_\tau S^a(2x+r, \tau) S^a(2x, 0) \rangle. \quad (23)$$

The zero-frequency Green's function $G_M(r)$ in turn is connected to the dynamical structure factor $S(q, \omega)$ via a Kramers-Kronig transform

$$G_M(r) = \frac{2}{\pi} \int_0^\infty d\omega' \int_0^{+\pi} dq S(q, \omega') \frac{\cos(qr)}{\omega'}. \quad (24)$$

Inserting the above equation into the definition of $A(r)$, Eq. (20), gives

$$A(r) = \frac{8}{\pi} \int_0^\infty d\omega' \int_0^\pi dq \cos^2 \frac{q}{2} S(q, \omega') \frac{\cos(qr)}{\omega'}. \quad (25)$$

Having related the interstitial exchange interactions \mathcal{J}_r to the dynamical structure factor, we evaluate numerically $S(q, \omega)$ in the subsequent sections to obtain precise estimates for the first few interstitial couplings $\mathcal{J}_1 \cdots \mathcal{J}_4$.

A. Two-spinon dynamical structure factor

First we compute the couplings \mathcal{J}_r using the two-spinon approximation for $S(q, \omega)$. The two-spinon contribution to the dynamical structure factor can be explicitly written as (see Refs. 53 and 54)

$$S_2(q, \omega) = \frac{1}{2\pi} \frac{e^{-I(\rho(q, \omega))}}{\sqrt{\omega_U^2(q) - \omega^2}} \Theta[\omega_q^U - \omega] \Theta[\omega_q^L - \omega], \quad (26)$$

with the fundamental integral

$$I(\rho) = \int_0^\infty dt \frac{e^t \cosh(2t) \cos(4\rho t) - 1}{t \cosh t \sinh(2t)}, \quad (27)$$

and with the lower continuum boundary $\omega_q^L = \frac{\pi}{2} \sin q$ and the upper continuum boundary $\omega_q^U = \pi \sin \frac{q}{2}$. The auxiliary variable ρ is a function of q and ω

$$\rho(q, \omega) = \frac{4}{\pi} \operatorname{acosh} \sqrt{\frac{\omega_U^2(q) - \omega_L^2(q)}{\omega^2 - \omega_L^2(q)}}. \quad (28)$$

Inserting $S_2(q, \omega)$ into formula (25), we obtain $A(r)$ in the two-spinon approximation

$$\begin{aligned} A_2(r) &= \frac{4}{\pi^2} \int_0^\pi dq \cos^2 \frac{q}{2} \cos(qr) \\ &\quad \times \int_{\omega_q^L}^{\omega_q^U} \frac{d\omega'}{\omega'} \frac{e^{-I(\rho(q, \omega'))}}{\sqrt{\omega_U^2(q) - \omega'^2}}. \end{aligned} \quad (29)$$

Expression (29) can be evaluated numerically in an efficient way, provided one splits off the singular part from integral (27) (see Ref. 53). In doing so, we obtain for the ratio between the couplings \mathcal{J}_2 and \mathcal{J}_1 the following result within the two-spinon approximation

$$\frac{\mathcal{J}_2}{\mathcal{J}_1} \simeq \frac{2A_2(2)}{A_2(1)} \simeq -0.7446, \quad (30a)$$

and find that \mathcal{J}_1 is ferromagnetic, while \mathcal{J}_2 is antiferromagnetic. Similarly, the magnitudes of further neighbor interactions are estimated to be

$$\frac{\mathcal{J}_3}{\mathcal{J}_1} \simeq +0.1909, \quad \frac{\mathcal{J}_4}{\mathcal{J}_1} \simeq -0.2312. \quad (30b)$$

with $\mathcal{J}_3 < 0$ and $\mathcal{J}_4 > 0$.

The two-spinon intensity accounts for about 73% of the total structure factor intensity.⁵³ The remaining part is carried by states with a higher number of spinons, and it is believed that the four-spinon intensity together with the two-spinon intensity cover about 98% of the spectral weight.⁵⁴ In principle, it would be possible to evaluate the ratios in Eq. (30) within the four-spinon approximation. However the involved numerical integrals are rather expensive to compute. Instead, we shall use finite size results for the structure factor to obtain a second estimate for the magnitude of the couplings \mathcal{J}_r .

B. Finite size results

We compute $A(r)$ using numerical data from the ABACUS database⁵⁵ for the dynamical structure factor in a finite system of $N = 500$ sites. These numerical data were obtained using a method based on the Bethe ansatz framework, which involves a summation over the so-called determinant representations for form factors of spin operators on the lattice.⁵⁶ In these computations the momentum delta functions are smoothed out

by including a finite broadening $\eta \sim 1/N$. Using the numerical data with a smearing $\eta = 0.01$ we obtain for the ratio $\mathcal{J}_2/\mathcal{J}_1$

$$\frac{\mathcal{J}_2}{\mathcal{J}_1} \simeq \frac{2A_N(2)}{A_N(1)} \simeq -0.7013, \quad (31a)$$

with $\mathcal{J}_1 < 0$ and $\mathcal{J}_2 > 0$, in accordance with Eq. (30a). The estimated magnitudes of further neighbor interactions are

$$\frac{\mathcal{J}_3}{\mathcal{J}_1} \simeq +0.2349, \quad \frac{\mathcal{J}_4}{\mathcal{J}_1} \simeq -0.1453, \quad (31b)$$

where \mathcal{J}_3 is ferromagnetic and \mathcal{J}_4 is antiferromagnetic. As anticipated from the RG treatment in Sec. IIIB, we observe that the magnitude of the coupling strengths decreases with spin separation distance.

Comparing Eqs. (30) to Eqs. (31), we infer that the values of $\mathcal{J}_2/\mathcal{J}_1$ agree well (within 10%), whereas the agreement between further neighbor interactions is worse. Since the two-spinon approximation misses 27% of the structure factor intensity, we suspect that the true values of the coupling strengths are closer to the finite size results (31) than to the two-spinon estimates. In the next section, we are going to work out the interstitial spin ordering using results (30) and (31) and neglecting any longer ranged interactions with $\mathcal{J}_{r>4}$.

V. SPATIALLY ANISOTROPIC TRIANGULAR LATTICE

As the discussions in the previous sections have shown, the ordering of the dangling spins \mathbf{s} , which occurs at an energy scale $O[(J')^2]$, is independent of the chain ordering. At the energy scale $O[(J')^2]$ the spins \mathbf{s} , which form a spatially anisotropic triangular lattice^{57,58,59,60}, are described by the effective Hamiltonian H_Δ , Eq. (10), with antiferromagnetic interactions along the horizontal bonds (J_2) and ferromagnetic interactions along the diagonal bonds (J_1), see Fig. 3. Neglecting third-nearest neighbor and longer ranged interactions, we can truncate the sums over r in Eq. (10) after the first two terms and obtain

$$H_\Delta \approx \mathcal{J}_1 \sum_{[ij]} \mathbf{s}_i \cdot \mathbf{s}_j + \mathcal{J}_2 \sum_{\langle ij \rangle} \mathbf{s}_i \cdot \mathbf{s}_j + \mathcal{J}_3 \sum_{[ij]'} \mathbf{s}_i \cdot \mathbf{s}_j + \mathcal{J}_4 \sum_{\langle ij \rangle'} \mathbf{s}_i \cdot \mathbf{s}_j, \quad (32)$$

where $[ij]$ and $[ij]'$ denote the diagonal bonds and $\langle ij \rangle$ and $\langle ij \rangle'$ the horizontal bonds connecting first and second-nearest neighbors, respectively (see Fig. 3). The values of the coupling strength $\mathcal{J}_1 \cdots \mathcal{J}_4$ are given by Eqs. (30,31).

This is a non-trivial spin-1/2 quantum model. However, it is also one which has been heavily studied, at least in the nearest-neighbor limit. In this case, over the vast majority of the phase diagram, the quantum ground state agrees with the classical one. This is particularly true when the couplings are such that the classical ground state is ‘‘close’’ to ferromagnetic (indeed the fully polarized ferromagnetic state is of course an

exact eigenstate, as usual). We therefore expect that a classical analysis is reliable, and pursue it below.

The classical phase diagram of Hamiltonian (32) is found by replacing the spin operators with classical coplanar spiral vectors,

$$\mathbf{s}_i = \hat{x} \cos(\mathbf{q} \cdot \mathbf{r}_i) + \hat{y} \sin(\mathbf{q} \cdot \mathbf{r}_i), \quad (33)$$

and minimizing the energy, which amounts to minimizing the Fourier transform of the exchange coupling^{61,62}

$$J(\mathbf{q}) = \sum_{i,j} \mathcal{J}_{i,j} \cos[\mathbf{q} \cdot (\mathbf{r}_i - \mathbf{r}_j)], \quad (34)$$

where \mathbf{r}_i denotes the position of site i in real space, and \hat{x} and \hat{y} are two orthogonal unit vectors. In our case, Eq. (34) gives

$$J(\mathbf{q}) = 2\mathcal{J}_1 \cos q_x \cos q_y + \mathcal{J}_2 \cos(2q_x) + 2\mathcal{J}_3 \cos(3q_x) \cos q_y + \mathcal{J}_4 \cos(4q_x). \quad (35)$$

with $J_1, J_3 < 0$ and $J_2, J_4 > 0$.

For simplicity, let us first analyze the minima of Eq. (35) for the case $\mathcal{J}_3 = \mathcal{J}_4 = 0$. This gives $\mathbf{q} = (q_x, 0)$ with

$$q_x = \begin{cases} 0, & \mathcal{J}_2 < |\mathcal{J}_1|/2, \\ \arccos[-\mathcal{J}_1/(2\mathcal{J}_2)], & \mathcal{J}_2 < |\mathcal{J}_1|/2. \end{cases} \quad (36)$$

That is, for $\mathcal{J}_2 < |\mathcal{J}_1|/2$ the classical ground state is ferromagnetic, whereas for $\mathcal{J}_2 > |\mathcal{J}_1|/2$ the ground state is a spiral state rotating along the x direction with the wave vector $\mathbf{q} = (q_x, 0)$. [To study how quantum fluctuations alter the classical ground state in the case $\mathcal{J}_3 = \mathcal{J}_4 = 0$ we have performed a linear spin-wave analysis (not shown). The magnetization decreases smoothly from 1/2 to zero as $\mathcal{J}_2/|\mathcal{J}_1|$ is increased, with a kink at $\mathcal{J}_2/|\mathcal{J}_1| = 1/2$.]

In the case of non-zero further neighbor interactions, $\mathcal{J}_3 \neq 0$ and $\mathcal{J}_4 \neq 0$, there is no simple explicit expression describing the global minima of $J(\mathbf{q})$, Eq. (35). Numerically we find that the minimum of $J(\mathbf{q})$ with the coupling values given by Eq. (31) (the finite size results) occurs at $\mathbf{q} = 0$, i.e., the ferromagnetic state is the ground state. However, the coupling parameters of Eq. (31) are rather close to the boundary of a spiral phase in the coupling parameter space $\{\mathcal{J}_r \mid r = 1, \dots, 4\}$. In particular, the coupling parameters in Eq. (30) (the two-spinon result) yield a spiral state with $\mathbf{q} \simeq 2\pi(0.08, 0)$. Therefore, we shall consider in what follows a cycloidal spiral ground state with wave vector $\mathbf{q} = (q_x, 0)$, with q_x small, which includes as a limiting case the ferromagnetic state ($q_x = 0$), that is,

$$\langle \mathbf{s}_{2x \pm \frac{1}{2}, 2y \mp \frac{1}{2}} \rangle = s_0 \left(\hat{x} \cos \left[2q_x x \pm \frac{q_x}{2} \right] + \hat{y} \sin \left[2q_x x \pm \frac{q_x}{2} \right] \right). \quad (37)$$

Here $s_0 \lesssim 1/2$ is the local static moment (staggered magnetization) of the spiral state.

VI. COUPLED HEISENBERG CHAINS IN A SPIRAL MAGNETIC FIELD

We are now in a position to address the spin-ordering pattern of the chains. We assume that the interstitial spins have

ordered into the spiral state given by Eq. (37), and focus on the lower temperature scale of order $(J')^4/J^3$, at which the chain spins become affected by relevant interchain interactions. The unperturbed system of antiferromagnetic Heisenberg chains is given by (note that we let $x \rightarrow x - 1/2$ compared to Sec. V)

$$H_0 = J \sum_{x,y} \mathbf{S}_{x-\frac{1}{2},y} \cdot \mathbf{S}_{x+\frac{1}{2},y}. \quad (38)$$

The perturbations are: (i) coupling between chain and interchain spins, described by (40), (ii) marginal ‘‘backscattering’’ term, which is already present for a single Heisenberg chain, and (iii) the fluctuation-generated interchain interactions (8).

Since the interchain spins form a two-dimensional ordered spiral state, described in the preceding section, the main effect of their interaction with the chain spins \mathbf{S} is described by the spiral magnetic field vector $\langle \mathbf{s}_x \rangle$ given by (note that we let $q_x \rightarrow q$ compared to Sec. V)

$$\langle \mathbf{s}_x \rangle = s_0 [\hat{x} \cos(qx) + \hat{y} \sin(qx)], \quad (39)$$

with q small. The spiral magnetic field introduces the following perturbations to this system of decoupled spins

$$H_S = J' \sum_{x,y} \left\{ \mathbf{S}_{2x-1/2,y} \cdot \langle \mathbf{s}_{2x-1} + \mathbf{s}_{2x} \rangle \right. \quad (40)$$

$$\left. + \mathbf{S}_{2x+1/2,y} \cdot \langle \mathbf{s}_{2x} + \mathbf{s}_{2x+1} \rangle \right\} \\ = \sum_{x,y} \mathbf{h}_{x+1/2} \cdot \mathbf{S}_{x+1/2,y}, \quad (41)$$

with

$$\mathbf{h}_x = 2h_0 \cos(q/2) [\hat{x} \cos(qx) + \hat{y} \sin(qx)], \quad (42)$$

and the field strength $h_0 = s_0 J'$.

The simplest effect of the spiral field, as for any field, is to induce a corresponding spiral magnetization in linear response. This implies that, generically, there will be static components of the chain spins in the spiral (x - y) plane. Since the spiral field is proportional to J' , and the chain susceptibility is generally proportional to $1/J$, these static components are of order J'/J .

This simple linear response, however, is not the complete story. A much more detailed analysis is needed to resolve the more subtle effects of the spiral field beyond linear response, in conjunction with the inter-chain couplings described in Sec. III. The nature of this more complete analysis depends crucially upon the magnitude of q . When q is small, the spins respond in a way which is similar to the response to a uniform magnetic field. A systematic approach is then possible, in which the Hamiltonian is transformed into the slowly rotating frame in which the external field is uniform. This is tractable because for small q the non-Heisenberg interactions induced by the change of frame are weak. Because of the expected smallness of q , we focus on this case in the remainder of this section.

In the opposite limit of a ‘‘large’’ wave vector, which is incommensurate with the dominant fluctuations of the 1D

Heisenberg chain, i.e. $q, |\pi - q| \sim O(1)$, the field weakly couples to the spin chain. Indeed, the leading $O(h)$ effects average out over space, and instead only sub-dominant terms are induced at $O(h^2)$. In this limit these weaker $O(h^2)$ terms are crucial in determining the final state of the system. Though this limit is actually conceptually simpler than the opposite one, it is technically challenging, because the effects of spiral field are determined by very short-wavelength properties of the Heisenberg spins. As a result, we are not unambiguously able to resolve the ground state in this limit. However, the ambiguity is small: we show in Appendix B that the system at zero temperature is in one of only *two* possible phases. One of these is the *same* non-coplanar state which we find in the small q limit (the other is a coplanar state). This supports the notion that, at least up to some critical $O(1)$ value of q (and possibly for all q), the ground state evolves smoothly from the small q limit.

A. Transformation to rotated frame

From here on, we assume $q \ll 1$. It is advantageous to rotate the chain spins towards the direction of the spiral magnetic field

$$\mathbf{S}_{x,y} \rightarrow \mathcal{R}_x \mathbf{S}_{x,y}, \\ \mathcal{R}_x = \begin{pmatrix} 0 & +\sin(qx) & -\cos(qx) \\ 0 & -\cos(qx) & -\sin(qx) \\ -1 & 0 & 0 \end{pmatrix}. \quad (43)$$

The rotation \mathcal{R}_x amounts to $-\pi/2$ rotation about the y axis followed by a rotation about the z axis with angle qx . We find that under rotation (43) the magnetic field term becomes

$$\tilde{H}_S = -2h_0 \cos(q/2) \sum_{x,y} S_{x+1/2,y}^z. \quad (44)$$

H_0 transforms into

$$H_0 = J \sum_{x,y} \left(S_{x-\frac{1}{2},y}^x S_{x+\frac{1}{2},y}^x + \cos q [S_{x-1/2,y}^y S_{x+1/2,y}^y \right. \\ \left. + S_{x-1/2,y}^z S_{x+1/2,y}^z] + \sin q [S_{x-1/2,y}^y S_{x+1/2,y}^z \right. \\ \left. - S_{x-1/2,y}^z S_{x+1/2,y}^y] \right). \quad (45)$$

In the limit of small q , which we focus on, this Hamiltonian is conveniently split into Heisenberg one \tilde{H}_0 with the modified exchange constant $\tilde{J} = J \cos q$,

$$\tilde{H}_0 = \tilde{J} \sum_{x,y} \mathbf{S}_{x-\frac{1}{2},y} \cdot \mathbf{S}_{x+\frac{1}{2},y}, \quad (46)$$

an effective Ising anisotropy \tilde{H}_1 along the x axis,

$$\tilde{H}_1 = J(1 - \cos q) \sum_{x,y} S_{x-\frac{1}{2},y}^x S_{x+\frac{1}{2},y}^x, \quad (47)$$

and an effective Dzyaloshinskii-Moriya (DM) interaction \tilde{H}_2

$$\tilde{H}_2 = J \sin q \sum_{x,y} \left[S_{x-1/2,y}^y S_{x+1/2,y}^z - S_{x-1/2,y}^z S_{x+1/2,y}^y \right] \quad (48)$$

Thus, $H_0 = \tilde{H}_0 + \tilde{H}_1 + \tilde{H}_2$.

1. Low-energy limit

It is appropriate now to take a low-energy limit, for which we use the non-Abelian spin current formulation. The zeroth-order Heisenberg Hamiltonian in the continuum limit yields the fixed point term plus a backscattering correction, $\tilde{H}_0 \rightarrow \tilde{H}_0 + H_{bs}$. The fixed point term, written in the Sugarawa form, is

$$\tilde{H}_0 = \frac{2\pi\tilde{u}}{3} \sum_y \int dx [\mathbf{J}_{L,y} \cdot \mathbf{J}_{L,y} + \mathbf{J}_{R,y} \cdot \mathbf{J}_{R,y}], \quad (49)$$

where $\tilde{u} = \cos qu$ is the modified spinon velocity. To the order we work in this section, it is sufficient to take $\tilde{u} \approx u = \pi J/2$. The backscattering correction is

$$H_{bs} = \sum_y \int dx \tilde{g}_{bs} \mathbf{J}_{L,y} \cdot \mathbf{J}_{R,y}, \quad (50)$$

where $\tilde{g}_{bs} = \cos qg_{bs} < 0$. Again we can approximate $\tilde{g}_{bs} \approx g_{bs}$ here.

The Ising anisotropy can also be expressed in terms of currents. One must take care since it is a composite operator. One obtains

$$\tilde{H}_1 = (1 - \cos q) \sum_y \int dx \left[\frac{2\pi u}{3} (J_{L,y}^x J_{L,y}^x + J_{R,y}^x J_{R,y}^x) + g_{bs} J_{R,y}^x J_{L,y}^x \right]. \quad (51)$$

The DM (see Ref. 63 for details) and external field \tilde{H}_S terms add up to

$$\tilde{H}_2 + \tilde{H}_S = \sum_y \int dx \left[\tilde{d} (J_{R,y}^x - J_{L,y}^x) - \tilde{h} (J_{R,y}^z + J_{L,y}^z) \right], \quad (52)$$

where $\tilde{d} = (3/\pi) \sin qJ$ and $\tilde{h} = 4h_0 \cos(q/2)$. We will consider both contributions in Eq. (52) on equal footing. Formally, we consider $q \ll 1$ and $J'/J \ll 1$, but with qJ/J' arbitrary. In this limit we may approximate $\tilde{J} \simeq J$, $\tilde{d} \simeq 3qJ/\pi$ and $\tilde{h} \simeq 2h_0$. Moreover, \tilde{H}_1 can be dropped completely, since it represents next, q^2 , order anisotropy corrections to both H_0 and the marginal backscattering term H_{bs} . (In principle, terms of order q^2 could be included by considering velocity shifts and small anisotropy corrections to the backscattering coupling g_{bs} . However, when q is small enough, these higher-order corrections will not affect the outcome of the analysis in an essential way.)

Finally, the relevant interchain interactions read

$$H'' = \sum_y \int dx \{ \gamma_N \mathbf{N}_y \cdot \mathbf{N}_{y+1} + \gamma_\varepsilon \varepsilon_y \varepsilon_{y+1} \}. \quad (53)$$

The analysis in Sec. III shows that coupling constants $\gamma_{N,\varepsilon}$ are of order $(J')^4/J^3$, and importantly, $\gamma_N > 0$.

B. Chiral SU(2) rotation

An unique feature of the WZNW field theory is its emergent *chiral* symmetry under independent SU(2) rotations for the left and right moving sectors. We take advantage of this to remove the DM term in Eq. (52). Specifically, we rotate the right and left chiral spin currents about the y axis by *opposite* angles, $+\theta$ and $-\theta$, respectively.

$$\mathbf{J}_{R,y} \longrightarrow \mathcal{R}_R \mathbf{J}_{R,y}, \quad \mathbf{J}_{L,y} \longrightarrow \mathcal{R}_L \mathbf{J}_{L,y}, \quad (54)$$

with

$$\mathcal{R}_{R/L} = \begin{pmatrix} \cos(\theta) & 0 & \mp \sin(\theta) \\ 0 & 1 & 0 \\ \pm \sin(\theta) & 0 & \cos(\theta) \end{pmatrix}, \quad (55)$$

where $\theta = +\text{atan}(\tilde{d}/\tilde{h})$. Under the rotations (54), the staggered magnetization and dimerization transform to

$$\begin{aligned} N_y^{x,z} &\rightarrow N_y^{x,z}, \\ N_y^y &\rightarrow \cos \theta N_y^y + \sin \theta \varepsilon_y, \\ \varepsilon_y &\rightarrow \cos \theta \varepsilon_y - \sin \theta N_y^y. \end{aligned} \quad (56)$$

Due to the chiral $SU(2)_R \times SU(2)_L$ symmetry, the low-energy \tilde{H}_0 Hamiltonian is unaffected. Vector perturbation (52) simplifies to \tilde{H}_z , where

$$\tilde{H}_z = -\sqrt{(\tilde{h})^2 + (\tilde{d})^2} \sum_y \int dx (J_{L,y}^z + J_{R,y}^z). \quad (57)$$

Under the rotation the back-scattering term transforms into

$$\begin{aligned} H_{bs} = \sum_{x,y} \left\{ \frac{g_1}{2} (J_{L,y}^+ J_{R,y}^- + J_{L,y}^- J_{R,y}^+) \right. \\ + \frac{g_2}{2} (J_{L,y}^+ J_{R,y}^+ + J_{L,y}^- J_{R,y}^-) + g_4 J_{L,y}^z J_{R,y}^z \\ \left. + \frac{g_3}{2} (J_{L,y}^z J_{R,y}^+ + J_{L,y}^z J_{R,y}^- - J_{L,y}^+ J_{R,y}^z - J_{L,y}^- J_{R,y}^z) \right\}, \end{aligned} \quad (58)$$

where the couplings g_i can be expressed in terms of the backscattering g_{bs}

$$\begin{aligned} g_1 = \frac{g_{bs}}{2} (1 + \cos 2\theta), \quad g_2 = \frac{g_{bs}}{2} (\cos 2\theta - 1), \\ g_3 = g_{bs} \sin 2\theta, \quad g_4 = g_{bs} \cos 2\theta. \end{aligned} \quad (59)$$

The interchain perturbation H'' is significantly affected as well, and now reads

$$\begin{aligned} H'' = \sum_{x,y} \left\{ \cos^2 \theta (\gamma_\varepsilon \varepsilon_y \varepsilon_{y+1} + \gamma_N N_y^y N_{y+1}^y) \right. \\ + \sin^2 \theta (\gamma_N \varepsilon_y \varepsilon_{y+1} + \gamma_\varepsilon N_y^y N_{y+1}^y) \\ + (\gamma_N - \gamma_\varepsilon) \cos \theta \sin \theta (\varepsilon_y N_{y+1}^y + N_y^y \varepsilon_{y+1}) \\ \left. + \gamma_N N_y^x N_{y+1}^x + \gamma_N N_y^z N_{y+1}^z \right\}. \end{aligned} \quad (60)$$

C. Absorption of the field h^z

The benefit of the chiral rotation is that within Abelian bosonization^{43,64,65} we can now absorb the magnetic field $h^z := \sqrt{(\tilde{h})^2 + (\tilde{d})^2}$ by the usual shift^{66,67}

$$\varphi_{s,y} \rightarrow \varphi_{s,y} + \frac{1}{\sqrt{2\pi}} \frac{h^z}{u} x, \quad (61)$$

for all y . Note that $h^z = J' \sqrt{(2s_0)^2 + (3qJ/\pi J')^2}$ is $O(J')$ in the scaling limit considered here [see the discussion after Eq. (50)].

This transforms the currents in the following way

$$J_{L,y}^\pm \rightarrow J_{L,y}^\pm e^{\pm i \frac{h^z}{u} x}, \quad J_{R,y}^\pm \rightarrow J_{R,y}^\pm e^{\mp i \frac{h^z}{u} x}, \quad (62)$$

$$J_{L,y}^z \rightarrow J_{L,y}^z + \frac{h^z}{4\pi u}, \quad J_{R,y}^z \rightarrow J_{R,y}^z + \frac{h^z}{4\pi u}. \quad (63)$$

The latter transformation explicitly embodies the linear response of the chain magnetization $M_y^z = J_{R,y}^z + J_{L,y}^z$ to the field.

The scaling dimension 1/2 fields transform according to

$$N_y^z \rightarrow \cos\left(\frac{h^z}{u} x\right) N_y^z + \sin\left(\frac{h^z}{u} x\right) \epsilon_y, \quad (64)$$

$$\epsilon_y \rightarrow \cos\left(\frac{h^z}{u} x\right) \epsilon_y - \sin\left(\frac{h^z}{u} x\right) N_y^z, \quad (65)$$

and N_y^x and N_y^y remain unchanged. Making this shift renders several terms in Eqs. (58,60) oscillatory, at scales $x > u/h^z$.

D. Renormalization group equations

Now we consider the effect of the various couplings. Because of the explicit oscillatory factors introduced by the shift in Eq. (61), we must consider two separate regimes of the flow. First, on scales shorter than the period of these oscillations, the oscillations themselves can be neglected, and we should consider all the couplings in Eqs. (58,60). On longer scales, the oscillatory couplings may be dropped entirely. The reader may be familiar with a similar treatment of the effects of a field on a Heisenberg chain by Affleck and Oshikawa.⁶⁶

1. Short-scale flows

Consider first the short-scale flows, i.e., the regime when $\frac{h^z}{u} e^\ell a_0 \lesssim 1$. This means

$$0 \leq \ell \lesssim \ell^* = \ln \frac{u}{h^z a_0} \sim \ln(J/J'). \quad (66)$$

We neglect completely the effect of the oscillatory factors induced in H_{bs} and H'' . Although the form in Eq. (58) is complicated, the flows remain simple. This is because Eqs. (58,59) are obtained from the chiral SU(2) rotation which is a symmetry of the fixed point Hamiltonian. Thus, since the field h^z has

no effect in this energy range, the flows remain fully SU(2) symmetric. They are simply

$$\frac{dg_{bs}}{d\ell} = \frac{[g_{bs}(\ell)]^2}{2\pi u}, \quad (67)$$

and

$$\frac{d\gamma_N}{d\ell} = \gamma_N - \frac{1}{4\pi u} g_{bs} \gamma_N, \quad (68)$$

$$\frac{d\gamma_\epsilon}{d\ell} = \gamma_\epsilon + \frac{3}{4\pi u} g_{bs} \gamma_\epsilon. \quad (69)$$

One can check this simple result by directly calculating the flow equations for $g_1 \cdots g_4$, and showing that the forms in Eqs. (59) are preserved by these equations. This is the result of the simple argument above.

We note that it is sufficient to work only to linear order in the relevant couplings $\gamma_N, \gamma_\epsilon$, since their initial values are of order $(J')^4$, and therefore remain small over this range of ℓ (they increase only by a factor of $e^\ell \sim J/J'$). To this order, they do not feed back into the flow of g_{bs} . The usual solution to Eq. (67) obtains:

$$g_{bs}(\ell) = \frac{g_{bs}}{\left(1 - \frac{g_{bs}}{2\pi u} \ell\right)}. \quad (70)$$

Since $g_{bs} < 0$, it becomes small under renormalization, and specifically of order u/ℓ for $\ell \gg 1$. Inserting this into the remaining equations and solving gives

$$\gamma_N(\ell) = \left(1 - \frac{g_{bs}\ell}{2\pi u}\right)^{1/2} e^\ell \gamma_N(0), \quad (71a)$$

$$\gamma_\epsilon(\ell) = \left(1 - \frac{g_{bs}\ell}{2\pi u}\right)^{-3/2} e^\ell \gamma_\epsilon(0). \quad (71b)$$

Evaluating this at $\ell = \ell^*$ and using Eqs. (16) for the initial conditions gives

$$\gamma_N(\ell^*) \sim \frac{1}{2\pi^4} \left(\frac{|g_{bs}| \ln(J/J')}{2\pi u}\right)^{1/2} \frac{(J')^3}{J^2}, \quad (72a)$$

$$\gamma_\epsilon(\ell^*) \sim -\frac{3}{4\pi^4} \left(\frac{|g_{bs}| \ln(J/J')}{2\pi u}\right)^{-3/2} \frac{(J')^3}{J^2}. \quad (72b)$$

Note that these couplings indeed remain small at this scale. Furthermore, the staggered magnetization coupling γ_N is already parametrically enhanced over the dimerization coupling γ_ϵ , by a factor of $\ln^2(J/J')$.

2. Long-scale flows

Now we consider the renormalization on scales longer than the period of the oscillations induced by the field shift. Here the SU(2) symmetry is truly broken, and the RG deviates from the simple one above. We drop all oscillating terms (this includes g_1, g_3 and several of the terms in H''), so that the re-

maining perturbations to the bare Hamiltonian \tilde{H}_0 are

$$\begin{aligned} H_{bs} &= \sum_{x,y} \left\{ \frac{\tilde{g}_2}{2} (J_{L,y}^+ J_{R,y}^+ + J_{L,y}^- J_{R,y}^-) + \tilde{g}_4 J_{L,y}^z J_{R,y}^z \right\}, \\ H'' &= \sum_{x,y} \left\{ \tilde{\gamma}_{N^y} N_y^y N_{y+1}^y + \tilde{\gamma}_{N^x} N_y^x N_{y+1}^x \right. \\ &\quad \left. + \tilde{\gamma}_+(N_y^z N_{y+1}^z + \varepsilon_y \varepsilon_{y+1}) \right\}, \end{aligned} \quad (73)$$

where we have introduced the new coupling constants $\tilde{g}_2, \tilde{g}_4, \tilde{\gamma}_{N^x}, \tilde{\gamma}_{N^y}, \tilde{\gamma}_+$. They should be matched at $\ell = \ell^*$ to the couplings from the short-scale flows, defined in Eqs. (60,58), which implies

$$\begin{aligned} \tilde{g}_2(\ell^*) &= -g_{bs}(\ell^*) \sin^2 \theta, \\ \tilde{g}_4(\ell^*) &= g_{bs}(\ell^*) \cos 2\theta, \\ \tilde{\gamma}_{N^x}(\ell^*) &= \gamma_N(\ell^*), \\ \tilde{\gamma}_{N^y}(\ell^*) &= \cos^2 \theta \gamma_N(\ell^*) + \sin^2 \theta \gamma_\varepsilon(\ell^*), \\ \tilde{\gamma}_+(\ell^*) &= [\cos^2 \theta \gamma_\varepsilon(\ell^*) + (1 + \sin^2 \theta) \gamma_N(\ell^*)] / 2. \end{aligned} \quad (74)$$

We now compute the RG equations for the perturbations (73) to the bare Hamiltonian H_0 using well-established OPEs for the non-Abelian spin currents (see for example Ref. 40). After some lengthy calculations we find

$$\begin{aligned} \frac{d\tilde{g}_2}{d\ell} &= -\frac{\tilde{g}_4 \tilde{g}_2}{2\pi u}, & \frac{d\tilde{g}_4}{d\ell} &= -\frac{\tilde{g}_2^2}{2\pi u}, \\ \frac{d\tilde{\gamma}_{N^x}}{d\ell} &= \left(1 - \frac{1}{4\pi u} \tilde{g}_4 + \frac{1}{2\pi u} \tilde{g}_2 \right) \tilde{\gamma}_{N^x}, \\ \frac{d\tilde{\gamma}_{N^y}}{d\ell} &= \left(1 - \frac{1}{4\pi u} \tilde{g}_4 - \frac{1}{2\pi u} \tilde{g}_2 \right) \tilde{\gamma}_{N^y}, \\ \frac{d\tilde{\gamma}_+}{d\ell} &= \left(1 + \frac{1}{4\pi u} \tilde{g}_4 \right) \tilde{\gamma}_+. \end{aligned} \quad (75)$$

It is important to understand how these equations lead to an instability. The equations for \tilde{g}_2, \tilde{g}_4 are decoupled, and can be solved separately. They have the standard form found in the Kosterlitz-Thouless (KT) analysis.⁴⁷ One recalls that the quantity

$$Y = \tilde{g}_2^2 - \tilde{g}_4^2 \quad (76)$$

is a constant of the motion. The flows are *unstable* provided $\tilde{g}_4(\ell^*) < |\tilde{g}_2(\ell^*)|$, which is *always* satisfied except when $\theta = \pi/2$ exactly, at which point it becomes an equality. That is for $\theta \in [0, \pi/2[$, the trajectories tend to $\tilde{g}_4 \rightarrow -\infty$ and $\tilde{g}_2 \rightarrow +\infty$. We fix Y by the initial conditions,

$$Y = |g_{bs}(\ell^*)|^2 (\sin^4 \theta - \cos^2 2\theta). \quad (77)$$

Hence, Y is negative for $\theta \in [0, \text{acos} \sqrt{2/3}]$ and positive for $\theta \in [\text{acos} \sqrt{2/3}, \pi/2]$. Writing $\tilde{g}_2^2 = Y + \tilde{g}_4^2$ we can solve the KT equations for \tilde{g}_4 . When $Y > 0$, i.e., in the crossover regime of the KT flow, we have

$$\text{atan} \left(\frac{\tilde{g}_4(\ell)}{\sqrt{Y}} \right) = \text{atan} \left(\frac{g_{bs}(\ell^*) \cos 2\theta}{\sqrt{Y}} \right) - \frac{\sqrt{Y}}{2\pi u} (\ell - \ell^*). \quad (78)$$

The coupling \tilde{g}_4 clearly diverges when the right-hand side of this equation reaches $\pi/2$ plus an integer times π . The ‘‘time’’ ℓ_d of this divergence is

$$\ell_d = \ell^* + \frac{2\pi u}{|g_{bs}(\ell^*)|} \frac{\pi/2 - \text{atan} \left(\frac{\cos 2\theta}{\Upsilon} \right)}{\Upsilon}, \quad (79)$$

where we define $\Upsilon = \sqrt{Y}/|g_{bs}(\ell^*)|$. Using $\ell^* \sim \ln(J/J')$ and $g_{bs}(\ell^*) \sim 2\pi u/\ell^*$ we obtain

$$\ell_d = \ln(J/J') \left[1 + \frac{\pi/2 - \text{atan} \left(\frac{\cos 2\theta}{\Upsilon} \right)}{\Upsilon} \right]. \quad (80)$$

One can check that $\ell_d/\ln(J/J')$ increases monotonically from 4 when $\theta = \text{acos} \sqrt{2/3}$ to infinity as $\theta \rightarrow \pi/2$. Similarly, when $Y < 0$ (strong-coupling regime) $\tilde{g}_4(\ell)$ diverges at the length scale

$$\ell_d = \ln(J/J') \left[1 + \text{atanh} \left(\frac{\bar{\Upsilon}}{\cos 2\theta} \right) (1/\bar{\Upsilon}) \right], \quad (81)$$

where $\bar{\Upsilon} = \sqrt{-Y}/|g_{bs}(\ell^*)|$. In this regime $\ell_d/\ln(J/J')$ takes the value 4 at $\theta = \text{acos} \sqrt{2/3}$, increases monotonically with decreasing θ , and diverges at $\theta = 0$.

With the values at $\ell = \ell^*$ given by Eqs. (72, 74) the relevant couplings $\tilde{\gamma}_{N^x}, \tilde{\gamma}_{N^y}$, and $\tilde{\gamma}_+$ become of order 1 at the length scale $\ell_o \sim 4 \ln(J/J')$ [so that $\ell_o - \ell^* \sim 3 \ln(J/J')$], which is always smaller than the scale ℓ_d . The most relevant of these turns out to be $\tilde{\gamma}_{N^x}$, as can be seen, e.g., by examining the ratio

$$\frac{\tilde{\gamma}_{N^x}(\ell)}{\tilde{\gamma}_{N^y}(\ell)} = \frac{\tilde{\gamma}_{N^x}(\ell^*)}{\tilde{\gamma}_{N^y}(\ell^*)} \exp \left[+ \frac{1}{\pi u} \int_{\ell^*}^{\ell} dx \tilde{g}_2(x) \right], \quad (82)$$

where (remember that $g_{bs} < 0$)

$$\tilde{g}_2(\ell^*) = |g_{bs}(\ell^*)| \sin^2 \theta = \frac{|g_{bs}(\ell^*)| \tilde{d}^2}{\tilde{d}^2 + \tilde{h}^2}. \quad (83)$$

From this clearly $\tilde{\gamma}_{N^x}$ becomes parametrically larger than $\tilde{\gamma}_{N^y}$ under renormalization (for $q \neq 0$). Similar analysis shows that $\tilde{\gamma}_{N^x}$ is also enhanced relative to $\tilde{\gamma}_+$. Thus, for $q > 0$, we find that the staggered magnetization $\tilde{\gamma}_{N^x} = \gamma_{N^x}$ dominates. Hence, the spins align antiferromagnetically along the x direction, \hat{S}_x^x , in the rotated (‘‘comoving’’) coordinate frame.

3. Ordering pattern of chain spins

Let us now infer what this means in terms of the original spins, in the fixed coordinate frame. It is necessary to trace back the transformations of the spin operators in Eqs. (43,54,61). This is straightforward but tedious. We will not give a general expression of the relation of the microscopic spins to the continuum operators after the final transformation, which is not illuminating. Instead, we give the result for the

expectation value of the spin operators given that, as argued above, in the rotated variables the ordering is very simple:

$$\langle N_y^a \rangle = M(-1)^y \delta^{a,x}, \quad (84)$$

$$\langle J_R^a \rangle = \langle J_L^a \rangle = \langle \epsilon \rangle = 0. \quad (85)$$

Here $M \neq 0$ represents the spontaneous moment, and will become the staggered magnetization. The $(-1)^y$ factor obtains because $\tilde{\gamma}_{N^x} > 0$.

Now we relate the spin operators as described above to the continuum fields:

$$\langle S_{x+\frac{1}{2},y}^x \rangle = -\frac{\hbar^z}{2\pi u} \cos \theta \cos qx, \quad (86)$$

$$\langle S_{x+\frac{1}{2},y}^y \rangle = -\frac{\hbar^z}{2\pi u} \cos \theta \sin qx, \quad (87)$$

$$\langle S_{x+\frac{1}{2},y}^z \rangle = -(-1)^{x+y} M. \quad (88)$$

Thus, indeed the dominating γ_{N^x} -term orders the chain spins antiferromagnetically along the z axis perpendicular to the x - y s -spiral plane. The non-zero components of the spins within the x - y plane are induced by the local field arising from the ordered interstitial moments. Note that they are of $O(J'/J)$ which is much larger than $M \sim (J'/J)^2$. Thus the static moments on the chains are predominantly in the plane of the spiral, with a smaller staggered component in the perpendicular (z) direction (see Fig. 2).

The case of *ferromagnetic* order amongst the interchain spins is obtained by setting $q = 0$. This implies $\tilde{d} = 0$ so that $\tilde{g}_2 = 0$, see (83). The chains are subjected to the uniform magnetic field \tilde{h} only. This leads to $\theta = 0$ and, as a result, symmetry in the $N^x - N^y$ plane: $\tilde{\gamma}_{N^x}/\tilde{\gamma}_{N^y} = 1$. The chain spins S order nearly collinearly with a ferromagnetic component of order $O(J'/J)$ and smaller antiferromagnetic component of order $O[(J'/J)^2]$ perpendicular to the ferromagnetic moments. Note that in this case, because the interstitial spins and the predominant moment of the chain spins are ferromagnetically ordered and hence collinear, the full magnetic order is actually *coplanar*. For instance, if the ferromagnetic moments are aligned in the \hat{x} direction, the antiferromagnetic component of the chain spins will be aligned along some axis \hat{e} in the y - z plane, and all the spins are contained in the plane spanned by \hat{x} and \hat{e} . Furthermore, this state is ferrimagnetic, i.e., has a macroscopic net moment, since the moments of the ferromagnetically ordered interstitial spins are unequal to the opposing in-plane component of the chain spin moments.

VII. SUMMARY AND DISCUSSION

In this work we have analyzed the ground state phase of the quantum Heisenberg antiferromagnet on the kagome lattice with spatially anisotropic exchange. We have studied this problem in the quasi-1D limit, where the lattice is broken up into antiferromagnetic spin-1/2 chains that are weakly interacting via intermediate ‘‘dangling’’ spins s (see Fig. 1). This limit lends itself to a perturbative RG analysis in the weak exchange interaction J' using bosonization and current algebra

techniques. We find that there is a natural separation of energy scales: the intermediate spins order at an energy scale of order $(J')^2/J$, at which the chains are not influenced by the interactions among themselves and with the interstitial spins. The low-energy behavior of the chains, on the other hand, is only modified at $O[(J')^4]$, as geometric frustration prevents the generation of relevant interchain interactions at the larger scale $(J')^2/J$. We have used perturbative and numerical methods to determine the effective interactions \mathcal{J}_i among the interstitial spins s , which arise at $O[(J')^2]$. It turns out that the spins s order in a coplanar cycloidal spiral with wave vector q parallel to the chain direction. The magnitude of the wave vector is presumably rather small (if not vanishing). It depends sensitively on the strength of further neighbor interactions among the interstitial spins, which cannot be reliably determined from our approach. The ordered interstitial moments induce a spiral order of the chain spins of $O(J'/J)$. Besides this, the chain spins exhibit a small antiferromagnetic component of $O[(J'/J)^2]$ that points along the axis perpendicular to the spiral plane. This *non-coplanar* ground state of the spatially anisotropic kagome antiferromagnet is illustrated in Fig. 2.

It is interesting to compare to recent results for this lattice in the spatially anisotropic limit. Wang *et al.*³⁸ found a coplanar ferrimagnetic chirality stripe order using a semiclassical analysis (see also Ref. 37). In this state, the interstitial spins are ferromagnetically ordered, and the chain spins are ordered in an antiferromagnetic fashion, nearly collinearly along an axis perpendicular to the interstitial moments, but canted slightly in that direction. The ordering of the interstitial spins is very close to our findings; i.e., it corresponds to the special case $q = 0$, which as we have described cannot be excluded by our calculations. However, even in this case the ordering pattern of the chain spins is quite different from that in Ref. 38, insofar as we find that the chain spins have a predominant *ferromagnetic* component antiparallel to the interstitial spins (and only a considerably smaller antiferromagnetic component perpendicular to the interstitial spins), while Wang *et al.*³⁸ obtained a predominantly *antiferromagnetic* ordering among the chain spins.

Yavors’kii *et al.* in Ref. 37, on the other hand, used a large- N expansion applied to the $\text{Sp}(N)$ -symmetric generalization of the model. In the limit $J' \ll J$ they found that the chains are completely decoupled, and the interstitial spins show some (short range) spin-spin correlation that is compatible with a spiral ordering pattern. While the mean field treatment of this large- N approach seems to miss the predominant spiral ordering of the chain spins, the spiral ordering of the interstitial spins is in agreement with the findings of this work.

Numerical studies of the spatially anisotropic kagome model should be very helpful in establishing the range of spatial anisotropy of exchange interaction where the non-coplanar ordered state found in this work represents the ground state of the system. We hope that our work will inspire further investigations of this interesting problem.

Acknowledgments

The authors thank J.-S. Caux for sharing his numerical data on the dynamical structure factor of the Heisenberg antiferromagnetic chain, and Ashvin Vishwanath and Fa Wang for conversations. This work was supported in part by the National Science Foundation under Grant No. PHY05-51164. A.P.S. thanks the Swiss National Science Foundation for its financial support. L.B. was supported by a David and Lucile Packard Foundation Fellowship and the NSF through DMR04-57440.

APPENDIX A: RG CALCULATIONS

In this Appendix we present a detailed derivation of flow equations (14) and (15) using standard OPE relations for the continuum fields.

1. Derivation of Eqs. (14)

The first order terms in the RG equations (14) originate from the rescaling of the time and space coordinates and the redefinition of the fields [see Eqs. (12)]. As already discussed in the main text, the interaction terms V_1 and V_2 , Eqs. (13), are local in space, which means that their scaling dimensions have to be compared with 1, the dimensionality of time τ . Interstitial spins have scaling dimension 0, while M (N) fields are of scaling dimension 1 (1/2). Consequently, the scaling dimension of V_1 is 1, while that of V_2 is 3/2, from which follows that the RG equation for the coupling γ_1 does not contain a linear term, while that for γ_2 starts with $(1 - 3/2)\gamma_2 = -\gamma_2/2$, in agreement with the first line of Eqs. (14).

The second and third lines of Eqs. (14) describe the flow of the fluctuation-generated interchain couplings V_{ch} , Eq. (8), and $V_{\text{ch}}^{(1)}$, Eq. (9), which operate in two-dimensional space-time. As a result, the scaling dimensions of the effective interchain interactions have to be compared with 2. The first order terms in the second line of Eqs. (14) are then a direct consequence of the fact that the scaling dimension of the $\gamma_{\partial N}$ -interaction is 3, while that of the γ_M -interaction is 2. Similarly, positive linear terms in the last line of Eqs. (14) follow from the *strong relevance* of the interchain couplings V_{ch} , Eq. (8), which have scaling dimension 1.

The second-order corrections to flow equations (14) are derived from contracting terms in perturbation expansion (11). In order to obtain the one-loop corrections in Eqs. (14), we need to consider contributions to the second order term in Eq. (11) that either yield a renormalization of the couplings γ_i or generate new *interchain* interactions. We begin by selecting from these contributions terms that contain a product of two intermediate spins from the same site, $(2x + \frac{1}{2}, y + \frac{1}{2})$,

say. These *local* contributions read

$$\begin{aligned} & \frac{1}{2} \Gamma \int d\tau_1 d\tau_2 s_{y+\frac{1}{2}}^a(\tau_1) s_{y+\frac{1}{2}}^b(\tau_2) \\ & \times \left(\gamma_1^2 [M_y^a(\tau_1) + M_{y+1}^a(\tau_1)] [M_y^b(\tau_2) + M_{y+1}^b(\tau_2)] \right. \\ & + 2\gamma_1\gamma_2 [M_y^a(\tau_1) + M_{y+1}^a(\tau_1)] \partial_x [N_y^b(\tau_2) + N_{y+1}^b(\tau_2)] \\ & \left. + \gamma_2^2 \partial_x [N_y^a(\tau_1) + N_{y+1}^a(\tau_1)] \partial_x [N_y^b(\tau_2) + N_{y+1}^b(\tau_2)] \right), \end{aligned} \quad (\text{A1})$$

where we have suppressed the x coordinate for brevity. Even though the interchain spins $s_{y+\frac{1}{2}}$ have no dynamics of their own at this level, they must be time-ordered as follows⁴⁸

$$\begin{aligned} & T s_{y+\frac{1}{2}}^a(\tau_1) s_{y+\frac{1}{2}}^b(\tau_2) \\ & = \theta_{\tau_1-\tau_2} s^a(\tau_1) s^b(\tau_2) + \theta_{\tau_2-\tau_1} s^b(\tau_2) s^a(\tau_1) \\ & = \frac{\delta^{ab}}{4} + \frac{i}{2} (\theta_t - \theta_{-t}) \epsilon^{abc} s^c(\tau), \end{aligned} \quad (\text{A2})$$

where θ_t is the step function, $\tau = (\tau_1 + \tau_2)/2$ is the center-of-mass time, and $t = \tau_1 - \tau_2$ is the relative time.

The off-diagonal term in Eq. (A2) (which is proportional to ϵ^{abc}) is responsible for the renormalization of the Kondo-like couplings γ_1 and γ_2 . As an example we consider the renormalization of γ_1 , which comes from the second line in Eq. (A1). Separating slow and fast degrees of freedom we can apply OPE (4) (and a similar expression for the left currents) to the product of two spin currents at nearby points [i.e., $M_y^a(\tau_1) M_y^b(\tau_2) \rightarrow i\epsilon^{abd} M_y^d(\tau)/(2\pi t)$]. Combining this with (A2) leads to

$$- \frac{\gamma_1^2}{4\pi u} \int d\tau s_{y+\frac{1}{2}}^c(\tau) M_y^c(\tau) \int_{\alpha < |t| < b\alpha} \frac{dt}{|t|}. \quad (\text{A3})$$

The integral with $|t| > b\alpha$ does not contribute to the renormalization. The one-loop correction to the flow equation for γ_1 can now be read off (A3) as $\propto d\ell \gamma_1^2/\pi u$, which gives us the first equation in (14).

The renormalization of γ_2 is computed in a similar way, one only needs to realize that it comes from the third line in Eq. (A1). Fusing M_y^a with $\partial_x N_y^b$ via the OPE (see Ref. 40 for more details)

$$\begin{aligned} & M_y^a(\tau_1) \partial_x N_y^b(\tau_2) = \lim_{x' \rightarrow x} M_y^a(x', \tau_1) \partial_x N_y^b(x, \tau_2) \\ & = \frac{-\delta^{ab} \varepsilon_y(x, \tau)}{2\pi(ut + a_0\sigma_t)^2} + \frac{i\epsilon^{abc} \partial_x N_y^c(x, \tau)}{2\pi(ut + a_0\sigma_t)}, \end{aligned} \quad (\text{A4})$$

leads to the following one-loop correction of the flow equation for γ_2 : $\delta\gamma_2 \propto d\ell \gamma_1 \gamma_2/\pi$. It is useful to note that rescaling of space and time does not affect quadratic terms, as each of them is explicitly proportional to the RG step $d\ell$, which comes from the shell integration of relative coordinates.

The second-order corrections to the flow equations for the interchain couplings γ_M and $\gamma_{\partial N}$ follow from the diagonal

term in Eq. (A2) (which is proportional to δ^{ab}). For example, applying relation (A2) to the second line of Eq. (A1) produces

$$\frac{\gamma_1^2}{4u} \int d\tau M_y^a(\tau) M_{y+1}^a(\tau) \int_{\alpha < |t| < b\alpha} dt.$$

To generate from this the γ_M term in Eq. (9) one needs to sum all local contributions like the one above using $\sum_x \dots = \int dx/(2a_0) \dots$, as appropriate for the kagome geometry. As a result one finds that $\gamma_M \sim \gamma_1^2 dl$. Similarly, the other interchain coupling, $\gamma_{\partial N}$ in Eq. (9), can be derived starting from the last line in Eq. (A1).

Finally, we turn to the relevant interchain interactions γ_N and γ_ε which are generated by fusing the marginal interaction γ_M and the irrelevant interaction $\gamma_{\partial N}$. Details of this procedure have been described previously in Refs. 39,40. Here we would only like to mention that the RG scheme that we have adopted here (i.e., integrating the one-loop x integrals over the *entire* space of relative x coordinates while restricting the relative time integral to the shell, $\alpha < |t| < b\alpha$), which is different from the RG scheme of Refs. 39,40, does not modify the outcome of the calculation in Refs. 39,40 in any significant way. Namely, upon fusing $M_y^a(x_1, \tau_1)$ with $\partial_x N_y^b(x_2, \tau_2)$ on chain y (and, similarly, on chain $y \pm 1$), one arrives at the following integral over the relative coordinate $x = x_1 - x_2$ and over relative time $t = \tau_1 - \tau_2$: $I \sim \int_{-\infty}^{\infty} dx \int_{\alpha < |t| < b\alpha} dt (x^2 + t^2)^{-2} \sim (b-1)\alpha^{-2}$. This explains the structure of the quadratic terms in the last line of Eqs. (14).

Additionally, we note that the third line in Eq. (A1) in combination with the first term in Eq. (A4) results in a strongly relevant contribution (scaling dimension 1/2)

$$\frac{-6\gamma_1\gamma_2}{\pi a_0 u} \int d\tau \varepsilon_y(x, \tau). \quad (\text{A5})$$

In the two-dimensional version of the spatially anisotropic kagome lattice this term cancels out, since the summation over local bow-tie crossings (that is, over x) brings in the factor $(-1)^x$ [which originates from the staggering factor in Eq. (2a)], resulting in $\int d\tau dx (-1)^x \varepsilon_y(x, \tau) \rightarrow 0$. This is how symmetry (3c) manifests itself.

In contrast, for the kagome *strip* of extension one in the y direction, the staggering factor $(-1)^x$ does not appear, since the bow-tie crossings are separated by *two* lattice spacings. As a consequence, the expression (A5) turns into $\int d\tau dx \varepsilon_y(x, \tau)$, which implies spontaneous dimerization of the kagome strip, an ordering pattern that does not reduce the translational symmetry. This strongly relevant term was missed in previous analytical work⁵⁰. Numerical studies, on the other hand, did find dimerized ground states⁵¹.

2. Derivation of Eq. (15)

To derive flow equation (15) we need to select from the second order term in Eq. (11) contributions that contain products of two different intermediate spins with the same y coordinate, $y + \frac{1}{2}$, say. Among these, the most important contributions are

those, that involve products of uniform or staggered magnetizations from the same chain

$$\begin{aligned} & +2 \times \frac{1}{2} \text{T} \sum_{x_1, x_2} \int d\tau_1 d\tau_2 s_{2x_1 + \frac{1}{2}}^a(\tau_1) s_{2x_2 + \frac{1}{2}}^b(\tau_2) \\ & \times \left[\gamma_1^2 M^a(2x_1, \tau_1) M^b(2x_2, \tau_2) \right. \\ & \left. + \gamma_2^2 \partial_x N^a(2x_1, \tau_1) \partial_x N^b(2x_2, \tau_2) \right], \quad (\text{A6}) \end{aligned}$$

where we have suppressed the y coordinate for brevity. The factor of 2 in the first line arises because there is an equal contribution from both the y and the $(y+1)$ chains. Since the spins $s_{2x+\frac{1}{2}}$ at different sites commute and time-ordering of the continuum fields M and N is automatic, we can disregard the operator T in the above expression, provided we exclude the case $x_1 = x_2$, which was treated in the previous subsection.

By splitting the integrals of Eq. (A6) into slow and fast degrees, we can use the OPEs, Eqs. (4), to fuse the product of two continuum fields at nearby points. In this way, we derive from Eq. (A6) the one-loop renormalization to the first term of the interaction H_Δ , Eq. (10)

$$\sum_{x_1, x_2} \int d\tau s_{2x_1 + \frac{1}{2}}^a s_{2x_2 + \frac{1}{2}}^a (\gamma_1^2 I_M^+ + \gamma_1^2 I_M^- + \gamma_2^2 I_N), \quad (\text{A7a})$$

with the integrals

$$I_M^\pm = \int_{\alpha < |t| < b\alpha} dt \frac{1/(8\pi^2)}{[ut \pm i(x_1 - x_2) + a_0\sigma_t]^2}, \quad (\text{A7b})$$

$$I_N = \int_{\alpha < |t| < b\alpha} dt \partial_{x_1} \partial_{x_2} \frac{C_N}{\sqrt{u^2 t^2 + 4(x_1 - x_2)^2}} \quad (\text{A7c})$$

where $C_N \approx (2\pi)^{-3/2}$ is the amplitude of the $\langle N^a N^a \rangle$ correlator. The integral over the infinitesimal interval $[\alpha, b\alpha]$ in Eqs. (A7b) and (A7c) amounts to replacing t with α_ℓ . The subsequent rescaling turns the cut-off α_ℓ back into the microscopic cut-off α , while $x \rightarrow x_\ell = x e^{-\ell}$. Simplifying $I_M = I_M^+ + I_M^-$ and explicitly taking derivatives in I_N leads to Eqs. (15). It is worth noting that the two contributions I_M and I_N are of opposite signs, resulting in a fast decay of interactions between interchain spins s .

APPENDIX B: CHAIN ORDERING IN THE LIMIT OF A LARGE SPIRAL WAVE VECTOR ($q \sim O[1]$)

In this Appendix, we briefly discuss how the chain spins might order under the perturbation of a spiral magnetic field with a large wave vector $\mathbf{q} = (q, 0)$, where $q \sim O[1]$. In this case the transformation to a rotated frame as done in Section VIA is not useful, as the generated interaction terms come with couplings of the order of the bare exchange J , see Eqs. (47) and (48). Instead, we should remain in the original, non-rotated basis, which leaves the dominant $O(J)$ interactions in their simplest form. Moreover, the rapid oscillation of the spiral field, which is highly incommensurate with the “natural” wave vectors 0 and π of correlations of the Heisenberg

chains, ensures that its effects rapidly average out to leading order. However, to $O(\hbar^2)$ we may expect non-oscillating interactions to be generated. In principle these can be obtained by a perturbative analysis expanding in powers of H_S (40).

As usual, symmetry analysis is helpful in figuring out the type of terms that can be expected from such a calculation. There are two important symmetries. First, the spiral field term breaks both spin-rotational and translational symmetries, but is invariant under a translation $x \rightarrow x + 1$ followed by a simultaneous spin rotation by the angle q about the z axis. Spiral state (39) is also invariant under spatial inversion ($x \rightarrow -x$) followed by a change of sign for the y and z components of the spins ($S^{y,z} \rightarrow -S^{y,z}$). Taking into account these constraints, the only possible marginal or relevant terms which may be generated in a single chain are

$$H_h^{(2)} = \sum_{xy} \int dx \{d_z(J_{yR}^z - J_{yL}^z) + \delta g_z J_{yR}^z J_{yL}^z\}. \quad (\text{B1})$$

We neglect here terms that are already present without the spiral field, and those that couple different chains as these coupling constants are necessarily smaller by at least one power of J' , since the latter cannot be generated without some bare inter-chain interactions.

A naive current algebra calculation using the continuum approximation, Eq. (2a) for the spin operators, indeed produces precisely these terms at $O(\hbar^2)$. However, the resulting explicit expressions are not reliable, as they are dominated by short distances of order q^{-1} , in which the continuum limit is inappropriate. A lattice scale calculation, similar in spirit to that in Sec. IV (yet more closely to that in Ref.⁴²), is required. Unfortunately, it turns out that to do so requires detailed information on the lattice scale properties of certain *four-spin* correlation functions of a Heisenberg chain. These data are not available to our knowledge. Therefore, we must rely upon the symmetry considerations alone, assuming no particular signs

or magnitudes for d_z and δg_z above, apart from the fact that both are expected to be of $O(\hbar^2/J)$.

Fortunately, this does not result in significant ambiguity. This is largely because the nominally “relevant” DM correction d_z has trivial effects. Similar to the magnetic field in (61) it can be removed by a simple shift. Unlike the case in Sec. III B, however, the shift does not affect the backscattering H_{bs} , which is written in terms of the field φ , which is dual to θ . The only effect of the shift is to change the ordering momentum, if any, of the $N^{x,y}$ components. It does not determine the nature of the ordering instability.

The anisotropy term δg_z is important, as it tips the balance of competition between different components of N fields in the interchain Hamiltonian H'' , Eq. (53). With the help of an OPE-based calculation similar to the one that led to Eq. (76) we find

$$\frac{d}{d\ell} \ln \frac{\gamma_{N^z}}{\gamma_{N^x}} = \frac{\delta g_z}{4\pi u}. \quad (\text{B2})$$

This tells us that the type of N -order is determined by the *sign* of the generated δg_z . Positive δg_z favors N^z components, leading to the non-coplanar ordering pattern found in Section VID 3, in the small- q limit. Negative δg_z , on the other hand, would prefer $N^{x,y}$ components, without breaking the symmetry between them. Such a state is clearly *co-planar*, and different from the one found in Section III B. Note that the DM term d_z will affect the ordering wave vector of this state but not the non-coplanar one. Which of these two situations is obtained cannot be discriminated by our analysis, since the sign of δg_z is not determined. However, it is rather natural to expect that as q is reduced from $O(1)$ values, one should observe behavior consistent with the small q analysis. This would suggest that $\delta g_z > 0$ for a non-vanishing range of q greater than zero, and indeed it is possible that this is the case for all q .

-
- ¹ D. A. Huse and A. D. Rutenberg, Phys. Rev. B **45**, 7536 (1992).
² A. V. Chubukov, Phys. Rev. Lett. **69**, 832 (1992).
³ P. Chandra, P. Coleman, and I. Ritchey, J. Phys. I **3**, 591 (1993).
⁴ J. N. Reimers, A. J. Berlinsky, Phys. Rev. B **48**, 9539 (1993).
⁵ C. Zeng and V. Elser, Phys. Rev. B **42**, 8436 (1990).
⁶ P. W. Leung and V. Elser, Phys. Rev. B **47**, 5459 (1993).
⁷ N. Elstner and A. P. Young, Phys. Rev. B **50**, 6871 (1994).
⁸ P. Lecheminant, B. Bernu, C. Lhuillier, L. Pierre, and P. Sindzingre, Phys. Rev. B **56**, 2521 (1997).
⁹ Ch. Waldtmann, H.-U. Everts, B. Bernu, C. Lhuillier, P. Sindzingre, P. Lecheminant, and L. Pierre, Eur. Phys. J. B **2**, 501 (1998).
¹⁰ P. Sindzingre, G. Misguich, C. Lhuillier, B. Bernu, L. Pierre, Ch. Waldtmann, and H.-U. Everts, Phys. Rev. Lett. **84**, 2953 (2000).
¹¹ G. Misguich and P. Sindzingre, Eur. Phys. J. B **59**, 305 (2007).
¹² R. R. P. Singh and D. A. Huse, Phys. Rev. Lett. **68**, 1766 (1992).
¹³ G. Misguich and B. Bernu, Phys. Rev. B **71**, 014417 (2005).
¹⁴ H. C. Jiang, Z. Y. Weng, and D. N. Sheng, arXiv:0804.1616v1 (unpublished).
¹⁵ M. Hermele, T. Senthil, and M. P. A. Fisher, Phys. Rev. B **72**, 104404 (2005).
¹⁶ Y. Ran, M. Hermele, P. A. Lee, and X.-G. Wen, Phys. Rev. Lett. **98**, 117205 (2007).
¹⁷ S. Ryu, O. I. Motrunich, J. Alicea, and M. P. A. Fisher, Phys. Rev. B **75**, 184406 (2007).
¹⁸ P. Nikolic and T. Senthil, Phys. Rev. B **68**, 214415 (2003).
¹⁹ R. Budnik and A. Auerbach, Phys. Rev. Lett. **93**, 187205 (2004).
²⁰ R. R. P. Singh and D. A. Huse, Phys. Rev. B **76**, 180407(R) (2007).
²¹ A. V. Syromyatnikov and S. V. Maleyev, Phys. Rev. B **66**, 132408 (2002).
²² A. V. Syromyatnikov and S. V. Maleyev, JETP **98**, 538 (2004).
²³ A. P. Shores, E. A. Nytko, B. M. Bartlett, and D. G. Nocera, J. Am. Chem. Soc. **127**, 13462 (2005).
²⁴ O. Ofer, A. Keren, E. A. Nytko, M. P. Shores, B. M. Bartlett, D. G. Nocera, C. Baines, and A. Amato, arXiv:cond-mat/0610540v1 (unpublished).
²⁵ J. S. Helton, K. Matan, M. P. Shores, E. A. Nytko, B. M. Bartlett, Y. Yoshida, Y. Takano, A. Suslov, Y. Qiu, J.-H. Chung, D. G. Nocera, and Y. S. Lee, Phys. Rev. Lett. **98**, 107204 (2007).

- ²⁶ P. Mendels, F. Bert, M. A. de Vries, A. Olariu, A. Harrison, F. Duc, J. C. Trombe, J. Lord, A. Amato, and C. Baines, *Phys. Rev. Lett.* **98**, 077204 (2007).
- ²⁷ T. Imai, E. A. Nytko, B. M. Bartlett, M. P. Shores, and D. G. Nocera, *Phys. Rev. Lett.* **100**, 077203 (2008).
- ²⁸ F. Bert, S. Nakamae, F. Ladieu, D. L'Hôte, P. Bonville, F. Duc, J.-C. Trombe, P. Mendels, *Phys. Rev. B* **76**, 132411 (2007).
- ²⁹ O. Ofer and A. Keren, arXiv:0804.4781v3 (unpublished).
- ³⁰ M. Rigol and R. R. P. Singh, *Phys. Rev. Lett.* **98**, 207204 (2007).
- ³¹ Z. Hiroi, M. Hanawa, N. Kobayashi, M. Nohara, H. Takagi, Y. Kato and M. Takigawa, *J. Phys. Soc. J.* **70**, 3377 (2001).
- ³² A. Fukaya, Y. Fudamoto, I. M. Gat, T. Ito, M. I. Larkin, A. T. Savici, Y. J. Uemura, P. P. Kyriakou, G. M. Luke, M. T. Rovers, K. M. Kojima, A. Keren, M. Hanawa, and Z. Hiroi, *Phys. Rev. Lett.* **91**, 207603 (2003).
- ³³ F. Bert, D. Bono, P. Mendels, J.-C. Trombe, P. Millet, A. Amato, C. Baines, and A. Hillier, *J. Phys.: Condens. Matter* **16**, S829 (2004).
- ³⁴ F. Bert, D. Bono, P. Mendels, F. Ladieu, F. Duc, J.-C. Trombe, and P. Millet, *Phys. Rev. Lett.* **95**, 087203 (2005).
- ³⁵ P. Sindzingre, arXiv:0707.4264v1 (unpublished).
- ³⁶ W. Apel, T. Yavors'kii, and H.-U. Everts, *J. Phys.: Condens. Matter* **19**, 145255 (2007); *J. Phys.: Condens. Matter* **19**, 349001 (2007).
- ³⁷ T. Yavors'kii, W. Apel, and H.-U. Everts, *Phys. Rev. B* **76**, 064430 (2007).
- ³⁸ F. Wang, A. Vishwanath, Y. B. Kim, *Phys. Rev. B* **76**, 094421 (2007).
- ³⁹ O. A. Starykh and L. Balents, *Phys. Rev. Lett.* **93**, 127202 (2004).
- ⁴⁰ O. A. Starykh, A. Furusaki, and L. Balents, *Phys. Rev. B* **72**, 094416 (2005).
- ⁴¹ O. A. Starykh and L. Balents, *Phys. Rev. Lett.* **98**, 077205 (2007).
- ⁴² E. M. Stoudenmire and L. Balents, *Phys. Rev. B* **77**, 174414 (2008).
- ⁴³ D. Sénéchal, *An introduction to bosonization*, cond-mat/9908262 (1999). Published in *Theoretical Methods for Strongly Correlated Electrons*, edited by D. Sénéchal, A.-M. Tremblay, and C. Bourbonnais (Springer, New York, 2003).
- ⁴⁴ J. von Delft and H. Schoeller, *Ann. Phys. (Leipzig)* **7**, 225 (1998).
- ⁴⁵ H.-H. Lin, L. Balents, and M. P. A. Fisher, *Phys. Rev. B* **56**, 6569 (1997).
- ⁴⁶ J. Cardy, in *Scaling and Renormalization in Statistical Physics*, Cambridge University Press (1996).
- ⁴⁷ A. O. Gogolin, A. A. Naersesyan, and A. M. Tsvelik, *Bosonization and Strongly Correlated Systems* (Cambridge University Press, Cambridge, U. K., 1998).
- ⁴⁸ I. Affleck, A. W. W. Ludwig, *Nucl. Phys. B* **360**, 641 (1991).
- ⁴⁹ S. Eggert, D. P. Gustafsson, and S. Rommer, *Phys. Rev. Lett.* **86**, 516 (2001).
- ⁵⁰ P. Azaria, C. Hooley, P. Lecheminant, C. Lhuillier, and A. M. Tsvelik, *Phys. Rev. Lett.* **81**, 1694 (1998). See also: P. Azaria, C. Hooley, P. Lecheminant, C. Lhuillier, and A. M. Tsvelik, *Phys. Rev. Lett.* **85**, 3331 (2000).
- ⁵¹ S. R. White and R. R. P. Singh, *Phys. Rev. Lett.* **85**, 3330 (2000).
- ⁵² A. Bohm, *Quantum Mechanics* (Springer-Verlag, New York, 1993).
- ⁵³ M. Karbach, G. Müller, A. H. Bougourzi, A. Fledderjohann, and K.-H. Mütter, *Phys. Rev. B* **55**, 12 510 (1997).
- ⁵⁴ J.S. Caux, R. Hagemans, *J. Stat. Mech.* 0612 (2006) P12013.
- ⁵⁵ *Algebraic Bethe ansatz computation of universal structure factors (ABACUS)*, see <http://staff.science.uva.nl/~jcaux/ABACUS.html>.
- ⁵⁶ J.S. Caux, R. Hagemans, and J.-M. Maillet, *J. Stat. Mech.* 0509 (2005) P09003.
- ⁵⁷ Th. Jolicoeur, E. Dagotto, E. Gagliano, and S. Bacci, *Phys. Rev. B* **42**, 4800 (1990).
- ⁵⁸ J. Merino, R. McKenzie, J. B. Marston and C. H. Chung *J. Phys.: Cond. Matt.* **11**, 2965 (1999).
- ⁵⁹ A. E. Trumper, *Phys. Rev. B* **60**, 2987 (1999).
- ⁶⁰ Z. Weihong, R. H. McKenzie, and R. R. P. Singh, *Phys. Rev. B* **59**, 14 367 (1999).
- ⁶¹ J. Villain, *J. Phys. Chem. Solids* **11**, 303 (1959).
- ⁶² Y. Yoshimori, *J. Phys. Soc. Jpn.* **14**, 807 (1959).
- ⁶³ S. Gangadharaiah, J. Sun, and O. A. Starykh, *Phys. Rev. B* **78**, 054436 (2008).
- ⁶⁴ R. Shankar, in *Current Topics in Condensed Matter and Particle Physics*, edited by Y. Lu, J. Pati, and Q. Shafi (World Scientific, Singapore 1993).
- ⁶⁵ N. Nagaosa, *Quantum field theory in strongly correlated electronic systems*, Springer (1998).
- ⁶⁶ I. Affleck and M. Oshikawa, *Phys. Rev. B* **60**, 1038 (1999).
- ⁶⁷ N.M. Bogoliubov, A.G. Izergin, and V.E. Korepin, *Nucl. Phys. B* **275**, 687 (1986).